Giant Meterwave Radio Telescope,
National Centre for Radio Astrophysics,
Tata Institute of Fundamental Research

Design Of Microstrip Bandpass Filters

STP 2007 Project Report

By,
Himanshu Madan,
College of Engineering, Pune

Guided by,
Mr. A. Praveen Kumar,
Engineer-F,
GMRT , NCRA

Acknowledgement

Working at Giant Meterwave Radio Telescope for my summer project for a second time, has been a very enriching experience for me. I am very thankful to Mr. A. Praveen Kumar, Engineer-F, GMRT, who has guided and supported me throughout my stint here. Technically as well as professionally, I have gained a lot through my association with him during my entire project work. I also would like to express my sincere gratitude to Mr. Anil Raut for providing me with much needed guidance regarding the computational component of the project, which required intensive analysis using softwares.

I would also like to take this opportunity to thank Mr. Vilas Bhalero, whose support has been indispensable throughout and specially in developing the protoype filter. I express my sincere gratitude to Mr. G. Shankar and Mrs. Manisha Parate for their cooperation throughout my project stage.

Gajenda Mulay and Santosh Bhor have been very helpful and cooperative during the project, many thanks to them. I also take this opportunity to thank my hostel inmates Avesh, Sandeep, Subhash, Sachin, Shelton, Raj and Shekher for all those colourful and memorable moments.

Himanshu Madan

Index

Contents **page no**

Chapter One
Introduction

Microwave filters are vital components in a huge variety of electronic systems, including mobile radio, Satellite Communication Receivers and Radar. Due to the advancement in the field of mobile and wireless communications, fully integrated analogue filters for high-frequency applications are now receiving great interest worldwide.

The use of microstrip in the design of microwave components and integrated circuits has gained tremendous popularity since the last decade because microstrips can operate in a wide range of frequencies. Furthermore, microstrip is lightweight, easy to fabricate and integrate in a cost effective way. Many researchers have presented numerous equations for the analysis and synthesis of microstrips. But with advent of various Full Wave EM Simulators the designing of Microwave structures have become easier.

This project deals with the designing and fabrication of different types of microstrip bandpass filters. The designing is done using AWR Microwave Office simulation program developed by Applied Wave Research USA. In the design of a Microwave filter using microstrips two types of design approaches are taken. First, transforming the lumped element design to equivalent planar structure. Second, using microstrip resonators and the concepts of immitance inverter. For the bandpass design the second approach is used.

Two types of filter design are dealt in this project. Hairpin Bandpass filter and Open Loop, Cross Coupled Bandpass filters. Hairpin filter has a Chebyshev response where as the Open Loop, Cross Coupled filter gives a elliptical response. With the help of the elliptical response Open Loop, Cross Coupled filter achieves a sharper cut off.

Chapter Two

Network Theory

Most of the RF and Microwave systems and devices can be modeled as a two port network. The two port representation basically helps in isolating either a complete circuit or a part of it and finding its characteristic parameters. Once this is done, the isolated part of the circuit, with a set of distinctive properties, enables us to abstract away its specific physical buildup, thus simplifying analysis. Any circuit can be transformed into a two-port network provided that it does not contain an independent source.

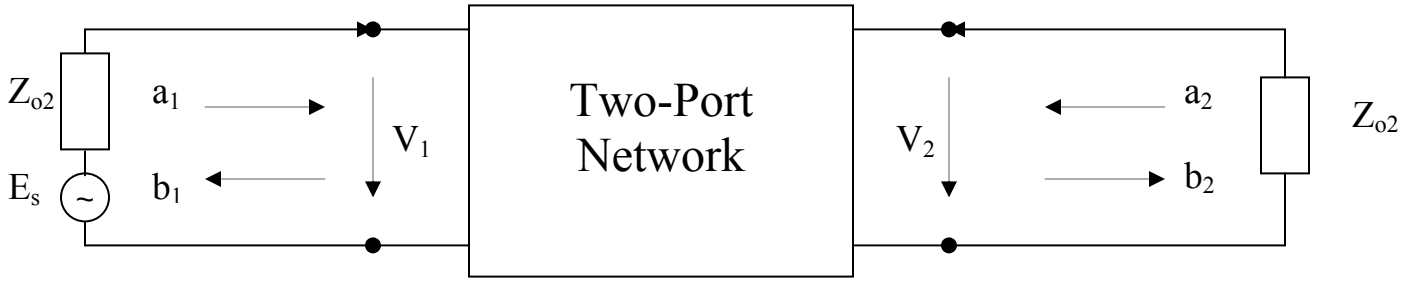

Figure 2.1: Two port network with its wave variables

Where V_1, V_2 and I_1, I_2 are the voltages and currents at respective ports and Z_{o1} and Z_{o2} are the terminal impedances. At RF and Microwave frequencies it is difficult to measure the voltages, thus new wave variables a_1, b_1 and a_2, b_2 are introduced with a signifying the incident wave and b implying the reflected wave.

The wave variables in terms of voltage and current are defined as follows

$$V_n = \sqrt{Z_{on}}\left(a_n + b_n\right)$$

$$I_n = \frac{1}{\sqrt{Z_{on}}}\left(a_n - b_n\right) \qquad \text{for n=1 and 2}$$

or

$$a_n = \frac{1}{2}\left(\frac{V_n}{\sqrt{Z_{on}}} + \sqrt{Z_{on}} I_n\right)$$

$$b_n = \frac{1}{2}\left(\frac{V_n}{\sqrt{Z_{on}}} - \sqrt{Z_{on}} I_n \right) \qquad \text{for n=1 and 2}$$

Which gives power at each port P_n

$$P_n = \frac{1}{2}\mathrm{Re}\left(V_n \cdot I_n^{*}\right) = \frac{1}{2}\left(a_n a_n^{*} - b_n b_n^{*}\right)$$

Now we will see few types of parameters used to define a two port network

2.1 Scattering Parameters

These are a set of parameters describing the scattering and reflection of traveling waves when a network is inserted into a transmission line. S- parameters are normally used to characterize high frequency networks, where simple models valid at lower frequencies cannot be applied. S-parameters are normally measured as a function of frequency, so when looking at the formulae for S-parameters it is important to note that frequency is implied, and that the complex gain (i.e. gain and phase) is also assumed. For this reason, S-parameters are often called complex scattering parameters.

$$S_{11} = \left.\frac{b_1}{a_1}\right|_{a_2=0} \qquad S_{12} = \left.\frac{b_1}{a_2}\right|_{a_1=0}$$

$$S_{21} = \left.\frac{b_2}{a_1}\right|_{a_2=0} \qquad S_{22} = \left.\frac{b_2}{a_2}\right|_{a_1=0}$$

S_{11} is the reflection coefficient of the input

S_{22} is the reflection coefficient of the output

S_{21} is the forward transmission gain

S_{12} is the reverse transmission gain

These definitions can also be written in a matrix form as

$$\begin{bmatrix} b_1 \\ b_2 \end{bmatrix} = \begin{bmatrix} S_{11} & S_{12} \\ S_{21} & S_{22} \end{bmatrix} . \begin{bmatrix} a_1 \\ a_2 \end{bmatrix}$$

2.2 Open Circuit Impedance Parameters

Impedance parameters are very useful in designing impedance matching and power distribution systems. Two port networks can either be voltage or current driven. For the current driven networks the input and output terminal voltage can be presented in matrix form as follows:

$$\begin{bmatrix} V_1 \\ V_2 \end{bmatrix} = \begin{bmatrix} Z_{11} & Z_{21} \\ Z_{21} & Z_{22} \end{bmatrix} . \begin{bmatrix} I_1 \\ I_2 \end{bmatrix}$$

Where the matrix which contain the z parameter is also called z matrix and is denoted by [z]

The z parameters for a two port network can be mathematically defined as

$$Z_{11} = \left. \frac{V_1}{I_1} \right|_{I_2=0} \qquad Z_{12} = \left. \frac{V_1}{I_2} \right|_{I_1=0}$$

$$Z_{21} = \left. \frac{V_2}{I_1} \right|_{I_2=0} \qquad Z_{22} = \left. \frac{V_2}{I_2} \right|_{I_1=0}$$

For reciprocal network $Z_{12} = Z_{21}$. For a symmetrical network $Z_{12} = Z_{21}$ and $Z_{11} = Z_{22}$. And for lossless network, the z parameters are imaginary.

2.3 Short-Circuit Admittance Parameters

Admittance parameters are very useful for describing the network when impedance parameters may not be existing. This is solved by finding the second set of parameters by expressing the terminal current in terms of the voltage. The input and output terminal current can be presented in matrix form as follows:

$$\begin{bmatrix} I_1 \\ I_2 \end{bmatrix} = \begin{bmatrix} Y_{11} & Y_{12} \\ Y_{21} & Y_{22} \end{bmatrix} . \begin{bmatrix} V_1 \\ V_2 \end{bmatrix}$$

Where the matrix which contain the y parameter is also called y matrix and is denoted by [y]

The Y parameters for a two port network can be mathematically defined as

$$Y_{11} = \left.\frac{I_1}{V_1}\right|_{V_2=0} \qquad Y_{12} = \left.\frac{I_1}{V_2}\right|_{V_1=0}$$

$$Y_{21} = \left.\frac{I_2}{V_1}\right|_{V_2=0} \qquad Y_{22} = \left.\frac{I_2}{V_2}\right|_{V_1=0}$$

For reciprocal network $Y_{12} = Y_{21}$. For a symmetrical network $Y_{12} = Y_{21}$ and $Y_{11} = Y_{22}$. And for lossless network, the y parameters are imaginary.

2.4 *ABCD* parameters

In *ABCD* parameter the input port voltage and current are considered variable and equation is formed in terms of the output voltage and current. The equation can be represented in matrix form as follows:

$$\begin{bmatrix} V_1 \\ I_1 \end{bmatrix} = \begin{bmatrix} A & B \\ C & D \end{bmatrix} \cdot \begin{bmatrix} V_2 \\ -I_2 \end{bmatrix}$$

The *ABCD* parameters for a two port network can be mathematically defined as

$$A = \left.\frac{V_1}{V_2}\right|_{I_2=0} \qquad B = \left.\frac{V_1}{-I_2}\right|_{V_2=0}$$

$$C = \left.\frac{I_1}{V_2}\right|_{I_2=0} \qquad D = \left.\frac{I_1}{-I_2}\right|_{V_2=0}$$

AD-BC=1 for reciprocal network

And *A=D* for symmetrical network

ABCD parameters are useful in analysis when the network can be broken into cascaded sub networks.

2.5 Important Definition

2.5.1 Insertion Loss

The loss resulting from the insertion of a network in a transmission line, expressed as the reciprocal of the ratio of the signal power delivered to that part of the line following the network to the signal power delivered to that same part before insertion. It is usually expressed in dB.

$$L_A = -20\log|S_{mn}| \text{ dB} \qquad m, n = 1, 2 \qquad (m \neq n)$$

where L_A denotes the insertion loss between the ports n and m.

2.5.2 Return Loss

The Return Loss of a line is the ratio of the power reflected back from the line to the power transmitted into the line. It is usually expressed in dB.

$$L_R = 20\log|S_{nn}| \text{ dB} \qquad n = 1, 2$$

2.5.3 Voltage Standing Wave Ratio

A standing wave may be formed when a wave is transmitted into one end of a transmission line and is reflected from the other end by an impedance mismatch. VSWR is the ratio of the maximum to minimum voltage in a standing wave pattern.

$$VSWR = \frac{1+|S_{nn}|}{1-|S_{nn}|} \qquad n = 1,2.$$

2.5.4 Phase Delay

Whenever we insert a sinusoid into a filter, a sinusoid must come out. The only thing that can change between input and output are the amplitude and the phase. Comparing a zero crossing of the input to a zero crossing of the output measures the so-

called phase delay. To quantify this we define an input, $\sin(\omega t)$ and an output $\sin(\omega t - \phi)$. Then the phase delay τ_p is found by solving

$$\sin(\omega t - \phi) = \sin \omega(t - \tau_p)$$

$$\omega t - \phi = \omega t - \omega \tau_p$$

$$\tau_p = \frac{\phi}{\omega} \text{ seconds}$$

Where ϕ is in radians and ω is in radians per second. The phase delay is actually the time delay for a steady sinusoidal signal and is not necessarily the true signal delay because a steady sinusoidal signal doesn't carry information.

2.5.5 Group Delay

Often the group delay is nothing more than the phase delay. This happens when the phase delay is independent of frequency. But when the phase delay depends on frequency, then a completely new velocity, the "group velocity" appears. Curiously, the group velocity is *not* an average of phase velocities.

The simplest analysis of group delay begins by defining a filter input x_t as the sum of two frequencies:

$$x_t = \cos \omega_1 t + \cos \omega_2 t$$

By using a trigonometric identity,

$$x_t = 2\cos\left(\frac{\omega_1 - \omega_2}{2} t\right)\cos\left(\frac{\omega_1 + \omega_2}{2} t\right)$$

We see that the sum of two cosines looks like a cosine of the average frequency multiplied by a cosine of half the difference frequency.

Each of the two frequencies could be delayed a different amount by a filter, so take the output of the filter y_t to be

$$y_t = \cos(\omega_1 t - \phi_1) + \cos(\omega_2 t - \phi_2)$$

In doing this, we have assumed that neither frequency was attenuated. (The group velocity concept loses its simplicity and much of its utility in dissipative media.) Using the same trigonometric identity, we find that

$$y_t = 2\cos\left(\frac{\omega_1 - \omega_2}{2}t - \frac{\phi_1 - \phi_2}{2}\right)\cos\left(\frac{\omega_1 + \omega_2}{2}t - \frac{\phi_1 + \phi_2}{2}\right)$$

Rewriting the beat factor in terms of a time delay t_g, we now have

$$\cos\left[\frac{\omega_1 - \omega_2}{2}(t - t_g)\right] = \cos\left(\frac{\omega_1 - \omega_2}{2}t - \frac{\phi_1 - \phi_2}{2}\right)$$

$$(\omega_1 - \omega_2)t_g = \phi_1 - \phi_2$$

$$t_g = \frac{\phi_1 - \phi_2}{\omega_1 - \omega_2} = \frac{\Delta\phi}{\Delta\omega}$$

For a continuum of frequencies, the *group delay* is

$$t_g = \frac{d\phi}{d\omega}$$

This represents the true signal (baseband signal) delay, and is also referred to as the envelope delay.

2.6 Immittance Inverter

Immittance Inverters are of two types, Impedance Inverter and Admittance inverter. The following Block diagram shows a Immittance Inverter.

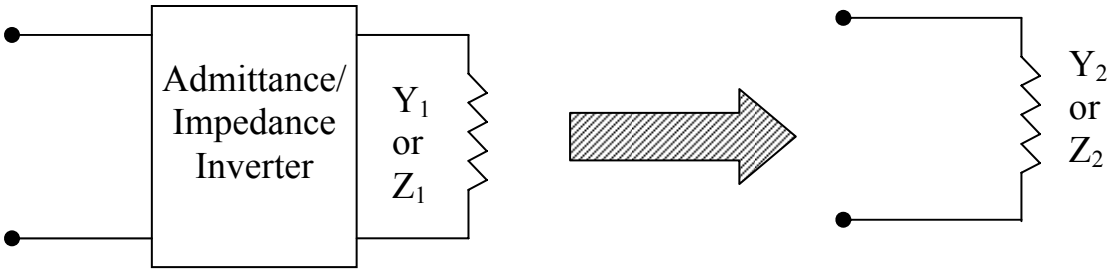

Figure 2.2: Immittance Inverter

An ideal *Impedance Inverter* is a two-port network that has a unique property at all frequencies, i.e. if it is terminated in impedance Z_1 on one port, the impedance Z_2 seen looking in the other port is

$$Z_2 = \frac{K^2}{Z_1}$$

where *K* is real and defined as characteristic impedance of the inverter. An impedance inverter converts a capacitance to inductance and vice versa. The ABCD matrix of the impedance inverter is

$$\begin{bmatrix} A & B \\ C & D \end{bmatrix} = \begin{bmatrix} 0 & \mp jK \\ \pm \frac{1}{jK} & 0 \end{bmatrix}$$

Similarly an ideal *Admittance Inverter* is a two-port network that if terminated in admittance Y_1 on one port, the impedance Y_2 seen looking in the other port is

$$Y_2 = \frac{J^2}{Y_1}$$

where *J* is real and defined as characteristic admittance of the inverter. Likewise an admittance inverter converts a capacitance to inductance and vice versa. The ABCD matrix of the admittance inverter is

$$\begin{bmatrix} A & B \\ C & D \end{bmatrix} = \begin{bmatrix} 0 & \pm \frac{1}{jJ} \\ \mp jJ & 0 \end{bmatrix}$$

Properties of Immitance Inverter

If a series inductance is present between two Impedance Inverters, it looks like a shunt capacitance from its exterior terminals.

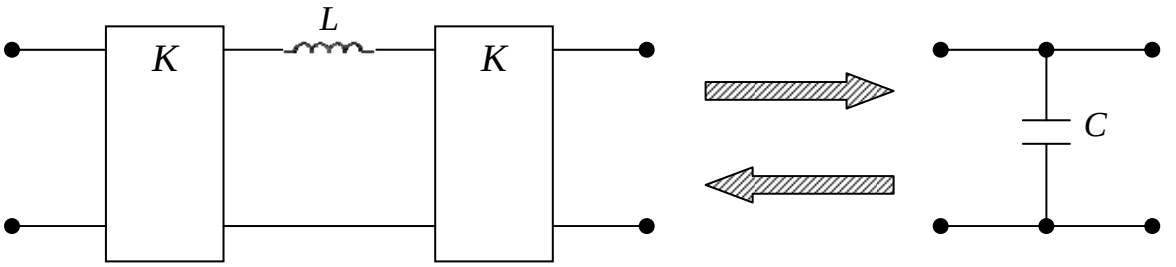

Figure 2.3: Immitance inverter used to convert a shunt capacitance into a equivalent circuit with series inductance.

Similarly if a shunt capacitance is present between two Admittance Inverters, it looks like a series inductance from its exterior terminals.

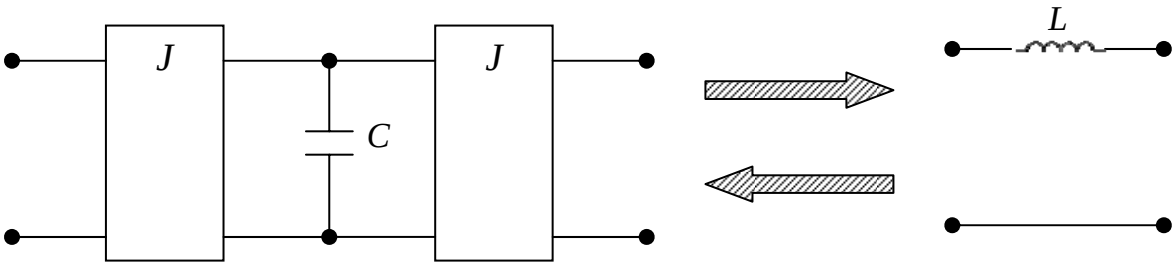

Figure 2.4: Immitance inverter used to convert a series inductance into a equivalent circuit with shunt capacitance.

Making use of the properties of Immittance Inverters, bandpass filters may be realized by series LC. resonant circuits separated by Impedance Inverters (*K*) or shunt LC. parallel resonant circuits separated by Admittance Inverters (*J*).

Chapter Three

Microstrip Basics

A general microstrip structure is shown in the figure 3.1, a microstip transmission line consists of a thin conductor strip over a dielectric substrate along with a ground plate at the bottom of the dielectric.

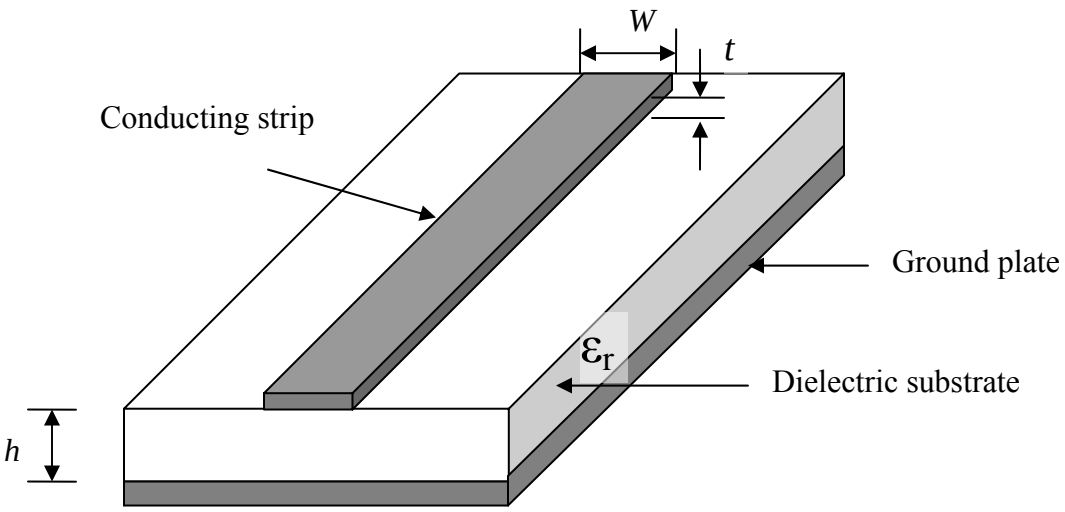

Figure 3.1: A basic Microstrip structure

3.1 Waves In Microstrip Line

Wave traveling in microstip line not only travel in the dielectric medium they also travel in the air media above the microstrip line. Thus they don't support pure TEM waves. In pure TEM transmission, the waves have only transverse component and the propagation velocity only depends on the permittivity and the permeability of the substrate. But in the case of microstrip line the magnetic and electric field also contain a longitudinal component, and their propagation velocity is dependent on the physical dimensions of the Microstrip as well.

If this longitudinal component is much smaller than the transverse component then the microstrip line can be approximated to TEM model. And this is called quasi TEM approximation.

3.2 Effective Dielectric Constant

Due to presence of two dielectric medium, air and the substrate, the effective dielectric constant replaces the relative dielectric constant of the substrate in the quasi TEM approximation. This effective dielectric constant is given in terms of $C_{d,}$ capacitance per unit length with the dielectric substrate present and C_a, capacitance per unit length with dielectric constant replaced by air and is given by

$$\varepsilon_{re} = \frac{C_d}{C_a}$$

The effective dielectric constant in terms of W (width of the Microstrip), h (height of the substrate) and ε_r (relative dielectric constant) given by Hammerstad and Jensen[5] is:

$$\varepsilon_{re} = \frac{\varepsilon_r + 1}{2} + \frac{\varepsilon_r - 1}{2}\left(1 + \frac{10}{u}\right)^{-ab}$$

where $u = \frac{W}{h}$, and

$$a = 1 + \frac{1}{49}\ln\left[\frac{u^4 + \left(\frac{u}{52}\right)^2}{u^4 + 0.432}\right] + \frac{1}{18.7}\ln\left[1 + \left(\frac{u}{18.1}\right)^3\right]$$

$$b = 0.564\left(\frac{\varepsilon_r - 0.9}{\varepsilon_r + 3}\right)^{0.053}$$

Accuracy of this model is 0.2% for $\varepsilon_r \le 128$ and $0.01 \le u \le 100$

3.3 Characteristic impedance

Characteristic impedance of the microstrip line is given by

$$Z_c = \frac{1}{c\sqrt{C_a C_d}}$$

where c is the velocity of electromagnetic waves in free space $c = 2.99 \times 10^8 m/s$.

Expression for characteristic impedance by hammerstad and Jensen[5] is

$$Z_c = \frac{\eta}{2\pi\sqrt{\varepsilon_{re}}} \ln\left[\frac{F}{u} + \sqrt{1+\left(\frac{2}{u}\right)^2}\right]$$

where $u = \frac{W}{h}$, $\eta = 120\pi$ ohms (free space impedance), and

$$F = 6 + (2\pi - 6)\exp\left[-\left(\frac{30.666}{u}\right)^{0.7528}\right]$$

The accuracy of $Z_c\sqrt{\varepsilon_{re}}$ is better than 0.01% for $u \le 1$ and 0.03% for $u \le 1000$

3.4 Some Other Formulae

3.4.1 *W/h*

For $W/h \le 2$

$$\frac{W}{h} = \frac{8\exp(A)}{\exp(2A) - 2}$$

with

$$A = \frac{Z_c}{60}\left\{\frac{\varepsilon_r + 1}{2}\right\}^{0.5} + \frac{\varepsilon_r - 1}{\varepsilon_r + 1}\left\{0.23 + \frac{0.11}{\varepsilon_r}\right\}$$

for $W/h \ge 2$

$$\frac{W}{h} = \frac{2}{\pi}\left\{(B-1) - \ln(2B-1) + \frac{\varepsilon_r - 1}{2\varepsilon_r}\left[\ln(B-1) + 0.39 - \frac{0.61}{\varepsilon_r}\right]\right\}$$

with

$$B = \frac{60\pi^2}{Z_c\sqrt{\varepsilon_r}}$$

3.4.2 Guided Wavelength

$$\lambda_g = \frac{\lambda_0}{\sqrt{\varepsilon_{re}}}$$

where λ_0 is the free space wavelength at frequency *f*.

3.4.3 Propagation Constant

$$\beta = \frac{2\pi}{\lambda_g}$$

3.4.4 Phase Velocity

$$v_p = \frac{\omega}{\beta} = \frac{c}{\sqrt{\varepsilon_{re}}}$$

3.4.5 Electrical Length

$$\theta = \beta l$$

θ is called the electrical length whereas *l* is the physical length of the microstrip. Thus, $\theta = \frac{\pi}{2}$ when $l = \frac{\lambda_g}{4}$ and $\theta = \pi$ when $l = \frac{\lambda_g}{2}$. These are called quarter wavelength and half wavelength microstrip line and are important in the filter design.

3.5 Effect of metal strip thickness

When the strip thickness *t* becomes comparable to the width of the substrate then its effect needs to be considered while designing. The following formulae show its effect on the characteristic impedance and effective dielectric constant.

For $W/h \le 1$

$$Z_c(t) = \frac{\eta}{2\pi\sqrt{\varepsilon_{re}}} \ln\left[\frac{8}{W_e(t)/h} + 0.25\frac{W_e(t)}{h}\right]$$

For $W/h \ge 1$

$$Z_c(t) = \frac{\eta}{\sqrt{\varepsilon_{re}}}\left[\frac{W_e(t)}{h} + 1.393 + 0.667\ln\left(\frac{W_e(t)}{h} + 1.444\right)\right]^{-1}$$

where

$$\frac{W_e(t)}{h} = \begin{cases} \frac{W}{h} + \frac{1.25}{\pi}\frac{t}{h}\left(1 + \ln\frac{4\pi W}{t}\right) & \frac{W}{h} \le 0.5\pi \\ \frac{W}{h} + \frac{1.25}{\pi}\frac{t}{h}\left(1 + \ln\frac{2h}{t}\right) & \frac{W}{h} \ge 0.5\pi \end{cases}$$

$$\varepsilon_{re}(t) = \varepsilon_{re} - \frac{\varepsilon_{re} - 1}{4.6}\frac{t/h}{\sqrt{W/h}}$$

where ε_{re} is the effective dielectric constant with t=0. It can be seen from the formulae that the effect of t is insignificant for small values of *t/h* ratio.

3.6 Surface Waves And Higher-Order Modes

Despite the absence of the top conductor there exists wave on ground plate guided by the air dielectric medium. These are called surface waves. The frequency at which these become significantly large is

$$f_s = \frac{c\tan^{-1}\varepsilon_r}{\sqrt{2}\pi h\sqrt{\varepsilon_r - 1}}$$

where the phase velocity of the two modes become equal.

To avoid excitation of higher-order modes in Microstrip the frequency of operation is kept below the cut off frequency

$$f_c = \frac{c}{\sqrt{\varepsilon_r}(2W + 0.8h)}$$

3.7 Coupled Lines

The following figure shows the cross section of a coupled line. Widely used in the construction of filters, they support two modes of excitation, even and odd mode.

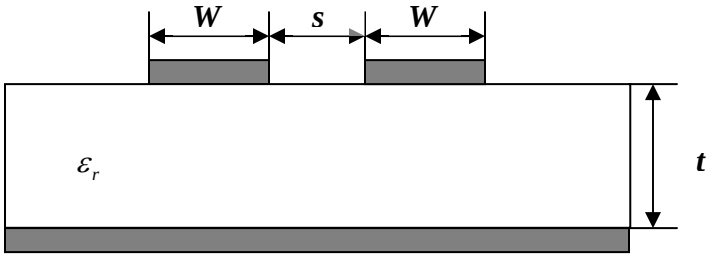

Figure 3.2: A Coupled Line Structure.

3.7.1 Even Mode

In even mode excitation both the microstrip coupled lines have the same voltage potential resulting in a magnetic wall at the symmetry plane

.

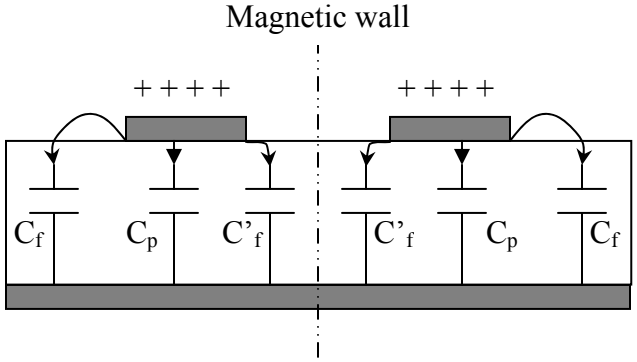

Figure 3.3: Quasi-TEM, Even Mode of a Pair of Coupled Microstrip Lines

Even mode capacitance is given by

$$C_e = C_p + C_f + C_f^{'}$$

where C_p is the parallel plate capacitance between the microstrip line and the ground plate. Hence

$$C_p = \varepsilon_0 \varepsilon_r \frac{W}{h}$$

C_f is the fringe capacitance and is given by

$$2C_f = \frac{\sqrt{\varepsilon_{re}}}{cZ_c} - C_p$$

And $C_f^{'}$ is the modified fringe capacitance, with the effect of the adjacent microstrip included.

$$C_f^{'} = \frac{C_f}{1 + A(h/s)\tanh(8s/h)}$$

where

$$A = \exp\left[-0.1\exp\left(2.33 - 2.53\,W/h\right)\right]$$

The even mode characteristic impedance can also be obtained from the capacitance

$$Z_{ce} = (c\sqrt{C_e C_e^a})^{-1}$$

where C_e^a is the even mode capacitance with air as a dielectric

And the effective dielectric constant for even mode is given as :

$$\varepsilon_{re}^e = \frac{C_e}{C_e^a}$$

3.7.2 Odd Mode

In odd mode the coupled microstrip line possess opposite potential. This results into a electric wall at the symmetry. The following cross section diagram shows the same.

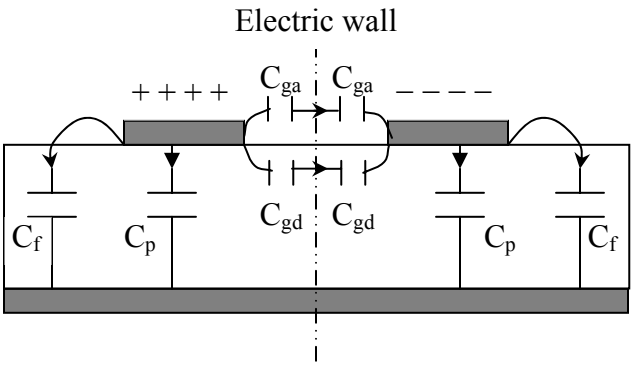

Figure 3.4: Quasi-TEM, Odd Mode of a Pair of Coupled Microstrip Lines

The resulting odd mode capacitance is given as

$$C_o = C_p + C_f + C_{gd} + C_{ga}$$

C_{ga} and C_{gd} represent fringe capacitance between the two microstrip line over the air and over the dielectric.

$$C_{ga} = \varepsilon_o \frac{K(k')}{K(k)}$$

where

$$k = \frac{s/h}{s/h + 2W/h}$$

$$k' = \sqrt{1 - k^2}$$

And the ratio of the elliptic function $\frac{K(k')}{K(k)}$ is given by

$$\frac{K(k')}{K(k)} = \begin{cases} \frac{1}{\pi} \ln\left(2\frac{1+\sqrt{k'}}{1-\sqrt{k'}}\right) & for 0 \le k^2 \le 0.5 \\ \frac{\pi}{\ln\left(2\frac{1+\sqrt{k}}{1-\sqrt{k}}\right)} & for 0.5 \le k^2 \le 1 \end{cases}$$

The odd mode characteristic impedance and effective dielectric constant is given as:

$$Z_{co} = (c\sqrt{C_o C_o^a})^{-1}$$

where C_e^a is the even mode capacitance with air as a dielectric.

$$\varepsilon_{re}^o = \frac{C_o}{C_o^a}$$

3.8 Lumped Elements to Microstrip Transform

The following figure shows a simple LC low pass filter circuit. At microwave frequencies the Microstrip lines act as inductor and capacitor. The Microstrip line has

both capacitance and inductance. If the Microstrip lines are made wide they have more capacitance and lower inductance and vice versa.

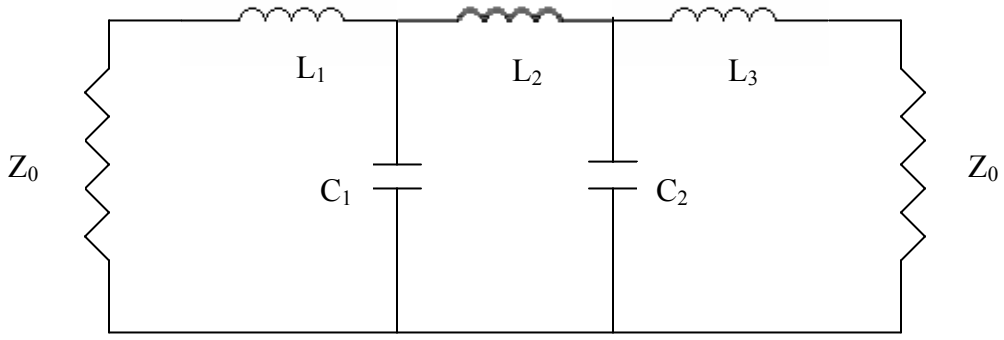

Figure 3.5: Lumped Element LC Lowpass Filter.

The following figure shows the equivalent microstrip realization of the lumped element filter.

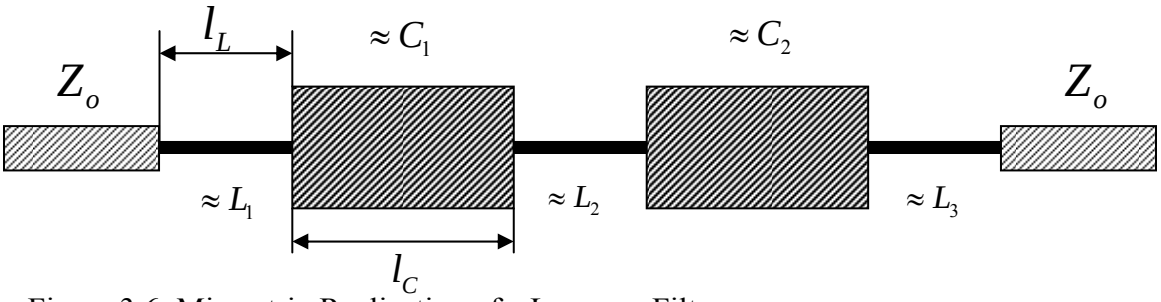

Figure 3.6: Microstrip Realization of a Lowpass Filter.

The important consideration while transforming is $Z_{0C} < Z_0 < Z_{0L}$, where Z_{0C} and Z_{0L} denote the characteristic impedances of the low and high impedance lines, respectively, and Z_0 is the source impedance, which is usually 50 ohms for microstrip filters.

A lower Z_{0C}, results in a better approximation of a lumped-element capacitor, but the resulting line width W, must not allow any transverse resonance to occur at operating frequencies.

A higher Z_{0L}, leads to a better approximation of a lumped-element inductor, but Z_{0L} must not be so high that its fabrication becomes inordinately difficult as a narrow line, or its current-carrying capability becomes a limitation.

The length of the capacitive and inductive microstrip lines can be calculated from the following equations

$$l_L = \frac{\lambda_{gL}}{2\pi}\sin^{-1}\left(\frac{\omega_c L}{Z_{0L}}\right)$$

$$l_C = \frac{\lambda_{gC}}{2\pi}\sin^{-1}\left(\omega_c C Z_{0C}\right)$$

where λ_{gL} and λ_{gC} are the guided wavelength of the inductive and capacitive microstrip line respectively and ω_c is the frequency of operation in radians. which is usually 50 ohms for microstrip filters. Although the above formulae takes into account the capacitive effect of the low-impedance line and the inductive effect of the high impedance line but it does not take into account the series reactance of the low-impedance line and the shunt susceptance of the high-impedance lines. To include these effects, the lengths of the high and low impedance lines should be adjusted to satisfy the following equations.

$$\omega_c L = Z_{0L}\sin\left(\frac{2\pi l_L}{\lambda_{gL}}\right) + Z_{0C}\tan\left(\frac{\pi l_C}{\lambda_{gC}}\right)$$

$$\omega_c C = \frac{1}{Z_{0C}}\sin\left(\frac{2\pi l_C}{\lambda_{gC}}\right) + 2\times\frac{1}{Z_{0L}}\tan\left(\frac{\pi l_L}{\lambda_{gL}}\right)$$

Chapter four

Hairpin Filter

Out of various bandpass microstrip filters, Hairpin filter is one of the most preferred one. The concept of hairpin filter is same as parallel coupled half wavelength resonator filters.

The advantage of hairpin filter over end coupled and parallel coupled microstrip realizations, is the optimal space utilization. This space utilization is achieved by folding of the half wavelength long resonators. Also the absence of any via to ground plane or any lumped element makes the design simpler. The following figure shows a typical hairpin structure.

(a) (b)

Figure 4.1: (a) tapped line input 5-pole Hairpin Filter (b) coupled line input 5-pole Hairpin Filter

4.1 Hairpin Resonator

Figure 4.2 shows a single Hairpin Resonator. α is called the slide angle. If the slide angle is small it might lead to coupling between the arms of individual resonator. The voltage at the end of hairpin arms is antiphase, and thus causes the arm to arm capacitance to have seemingly disproportionate effect. The added capacitance lowers the resonant frequency requiring a shortening of the hairpin to compensate.

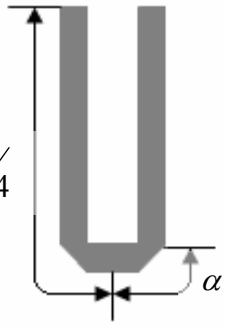

Figure 4.2: Hairpin Resonator

To avoid this, slide angle is kept as large as possible. But by increasing the slide angle the coupling length between two resonators reduces, so as to attain the required coupling, the coupling spacing needs to be

reduced which posses a practical limitation. For practical design purpose slide angle is kept twice the strip width to avoid inter-element coupling.

4.2 Tapped line input

Conventional filters employ coupled line input. Tapped line input has a space saving advantage over coupled line input. Further while designing sometime the coupling dimensions required for the input and output coupled line is very small and practically not achievable which hinders the realizability of the design. Thus tapped line input is preferred over coupled line input.

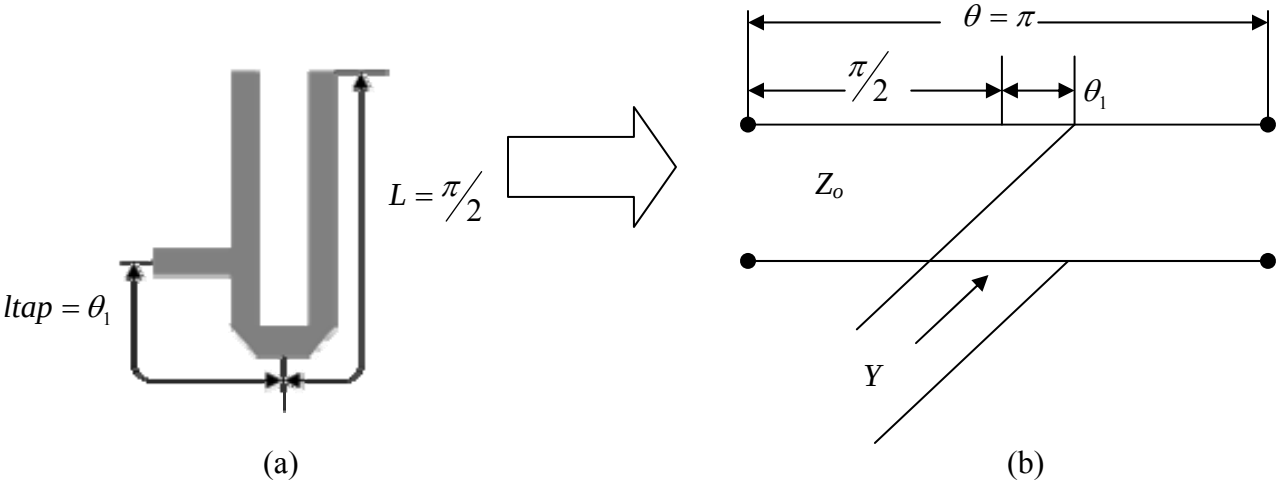

Figure 4.3: (a) Tapped Hairpin Resonator Schematic. (b) Equialent Circuit of a Tapped Hairpin Resonator

Assuming negligible coupling between the arms of the hairpin resonator, the input admittance at the tap point can be given as

$$Y = G + jB = \frac{\pi Y_0}{2\sin^2\theta_1}\left(\frac{1}{Q_e} + j2\frac{f - f_0}{f_0}\right)$$

provided that

$$\left|\frac{f - f_0}{f_0}\right| << 1$$

And

$$\left[\frac{\theta(f-f_0)}{f_0}\right]\cot\theta_1 << 1$$

where f_0 is the resonant frequency, f is the instantaneous frequency , Q_e is singly loaded Q and $Z_0=1/Y_0$ is the characteristic impedance of the hairpin resonator. Comparing the real part singly loaded Q can be obtained as

$$Q_e = \frac{R}{Z_0}\frac{\pi}{2\sin^2\theta_1}$$

where $R=1/G$.

4.3 Design Parameter For Hairpin Filter

For Designing a Hairpin filter, Full Wave EM simulation is used. For the design purpose the low pass prototype (Butterworth, Chebyshev, Bessel)[Appendix A] is selected according to the design requirement.

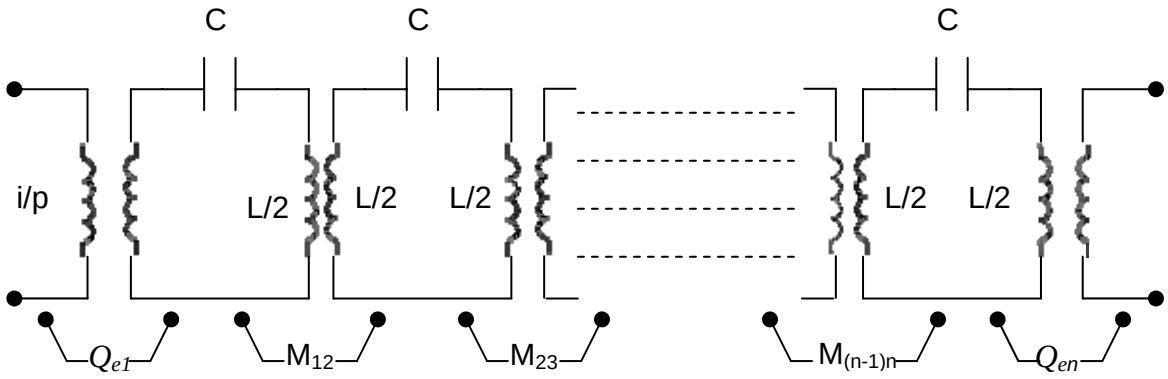

Figure 4.4: Equivalent circuit of the n-pole Hairpin Bandpass Filter

As seen from the equivalent circuit of n pole Hairpin filter, each resonator can be modeled as a combination of inductor and capacitor. The mutual coupling coefficient between two resonators is $M_{i+1,i}$. Q_{e1} and Q_{en} are the Quality Factor at the input and output.

Coupling coefficient and Quality Factor can be calculated as

$$Q_{e1} = \frac{g_0 g_1}{FBW}$$

$$Q_{en} = \frac{g_n g_{n+1}}{FBW}$$

$$M_{i,i+1} = \frac{FBW}{\sqrt{g_i g_{i+1}}} \qquad \text{for } i = 1 \text{ to } n\text{-}1$$

where FBW is the fractional bandwidth and $g_{0,1.....n+1}$ are the normalized lowpass element of the desired low pass filter approximation.

The quality factor can be substituted and the *ltap* length can be calculated as

$$ltap = \frac{2L}{\pi} \sin^{-1}\left(\sqrt{\frac{\pi}{2} \frac{Z_0 / R}{Q_e}} \right)$$

$$2L = \frac{\lambda_g}{2} = \frac{\lambda_o}{2\sqrt{\varepsilon_{re}}} = \frac{C}{2 f_0 \sqrt{\varepsilon_{re}}}$$

Chapter Five

Open Loop, Cross coupled Planar Filter

When the frequency selectivity and low band pass loss are considered to be the prime importance then elliptical filters are employed. Elliptical filters exhibit equi-ripple response in both passband and stopband.

Simple concept of multipath propagation is used to cancel out signals and to obtain transmission zero at finite frequency or group delay flattening or both simultaneously. Although such multipath filters are realized using waveguide cavities or dielectric resonator loaded cavities, because of their low insertion loss can also be developed as planar structure. This is achieved by employing cross coupling between two nonadjacent resonator.

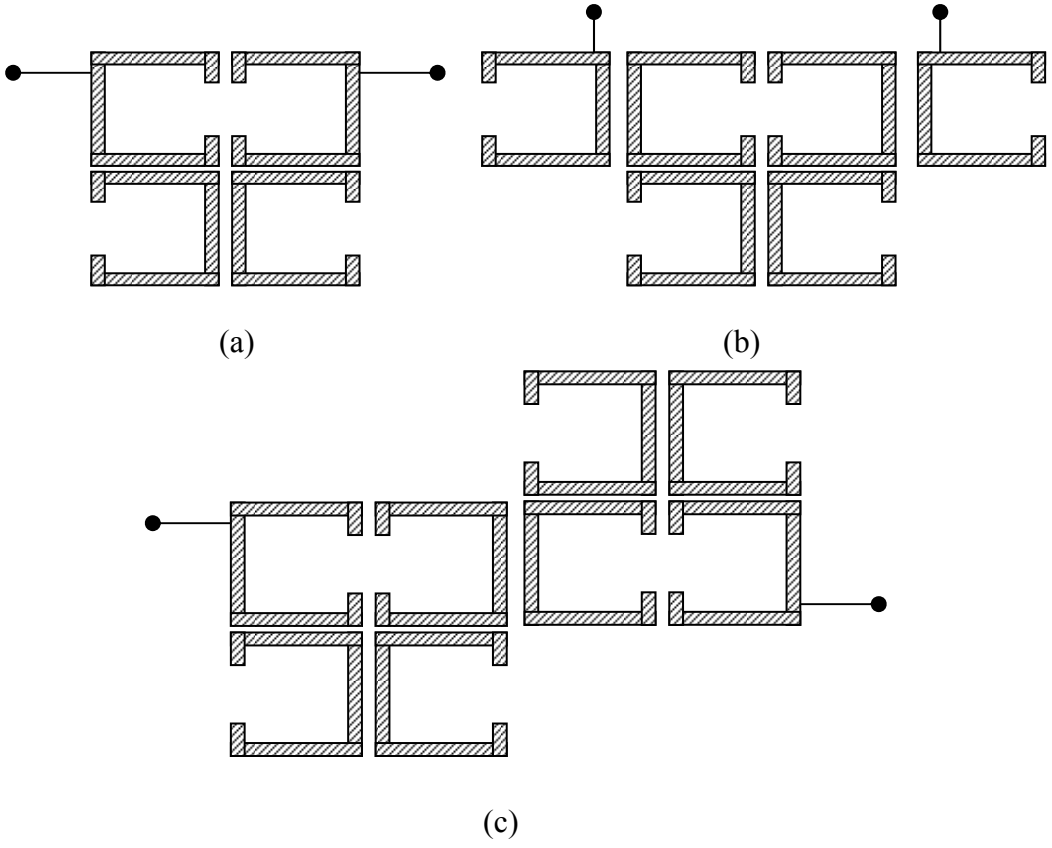

Figure 5.1: (a) Four Pole (b) Six Pole (c) Eight Pole cross coupled planar microwave bandpass filters.

5.1 Four pole Open Loop, Cross Coupled Bandpass Filter

The low pass prototype of the filter can be seen in the figure below. The cross coupling can be seen with the admittance inverter J_1. The value of J_1 decides the location of transmission zero.

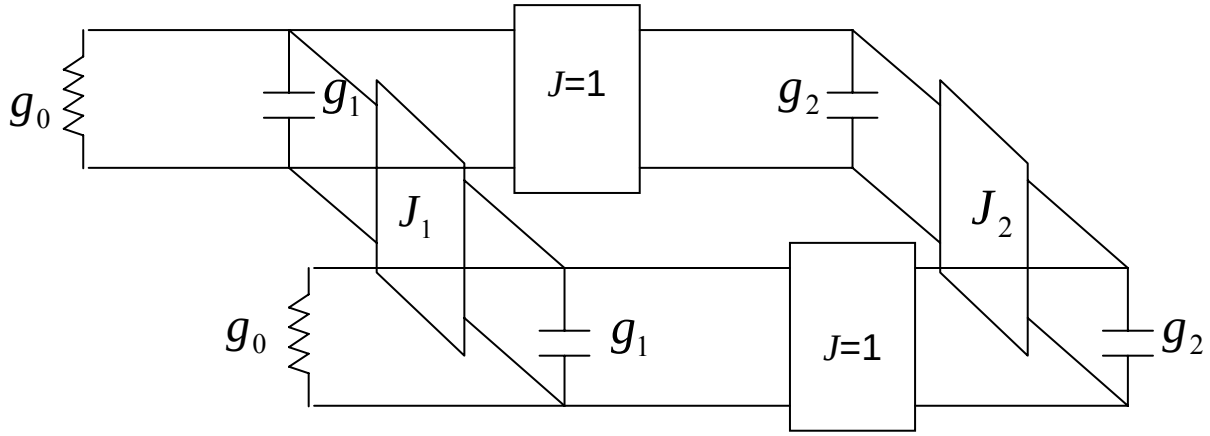

Figure 5.2: Lowpass Prototype of Four pole Open Loop, Cross Coupled Filter.

The value of low pass prototype component can be calculated from the following formulae as described in [].

$$g_1 = \frac{2\sin\frac{\pi}{2n}}{\gamma}$$

$$g_2 g_1 = \frac{4\sin\frac{3\pi}{8}\sin\frac{1}{8}}{\gamma^2 + \sin^2\frac{\pi}{4}}$$

$$\gamma = \sinh\left(\frac{1}{4}\sinh^{-1}\frac{1}{\varepsilon}\right)$$

$$S = \left(\sqrt{1+\varepsilon^2} + \varepsilon\right)^2 \qquad \text{(the passband VSWR)}$$

For Chebyshev response the cross coupling can be eliminated and thus the admittance inverters become:

$$J_1 = 0$$

$$J_2 = \frac{1}{\sqrt{S}}$$

For elliptical filter in order to introduce a transmission zero at $\omega = \pm\omega_a$, the required value of J_1 is given by

$$J_1 = \frac{-J_2^{'}}{(\omega_a g_2)^2 - J_2^{'2}}$$

and the modified J_2

$$J_2^{'} = \frac{J_2}{1 + J_2 J_1}$$

5.2 Design Parameter for Four pole Open Loop, Cross Coupled Bandpass Filter

The low pass filter prototype can be converted to the required bandpass filter design. The equivalent circuit diagram for the planar filter is given below. $M_{12,}$ M_{23} and M_{34} are the mutual coupling coefficient between the adjacent resonators. The M_{14} is the mutual coupling coefficient between the nonadjacent resonator 1 and 4.

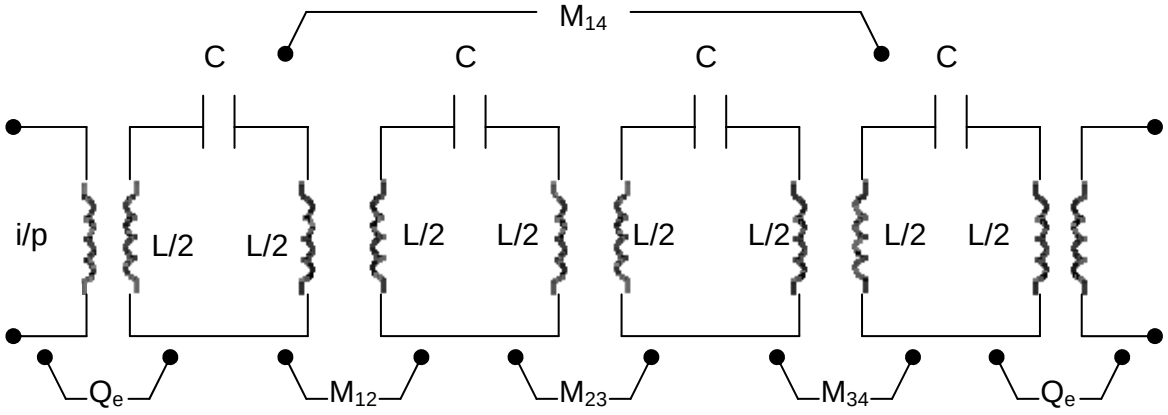

Figure: Equivalent circuit of the Four pole Open Loop, Cross Coupled Bandpass Filter.

$$Q_e = \frac{g_0 g_1}{FBW}$$

$$M_{12} = M_{34} = \frac{FBW}{\sqrt{g_1 g_2}}$$

$$M_{23} = \frac{FBW \cdot J_2}{g_2}$$

$$M_{14} = \frac{FBW \cdot J_1}{g1}$$

where *FBW* is the fractional bandwidth.

Chapter Six

Coupling of Microstrip Resonators

Coupling of two resonators is the primary component of a bandpass filter design. Coupling between two resonators is basically due to the fringe fields. The nature and the extent of these fringes determine the strength and thtype of coupling. There are three types of basic coupling, electric coupling, magnetic coupling and mixed coupling involving both electric and magnetic coupling. In the subsequent sections we will analyze square open loop resonators for various coupling properties.

6.1 Coupling Coefficient

Coupling coefficient is a dimensionless quantity. It is defined as the ratio of coupled energy to stored energy in the resonator. It can be mathematically given as

$$k_e = \frac{C_m}{C} \qquad \text{electric coupling coefficient}$$

where C_m is the mutual capacitance between the two resonator and C is the self capacitance of the resonator

$$k_m = \frac{L_m}{L} \qquad \text{magnetic coupling coefficient}$$

where L_m is the mutual inductance between the two resonator and L is the self inductance of the resonator

6.2 Electric Coupling

At resonance, the open loop resonator has the maximum electric field density at the side with an open gap. This is because the fringe field at the open end is the strongest. Thus an electric coupling can be achieved by having the sides with open gap proximately placed. Thus the planar structure shown in the figure exhibit electric coupling.

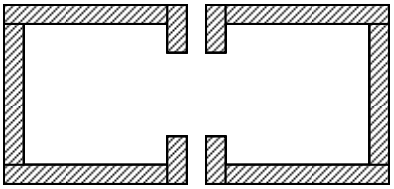

Figure 6.1: Electric Coupling Structure

The equivalent circuit of the planar structure can be drawn as

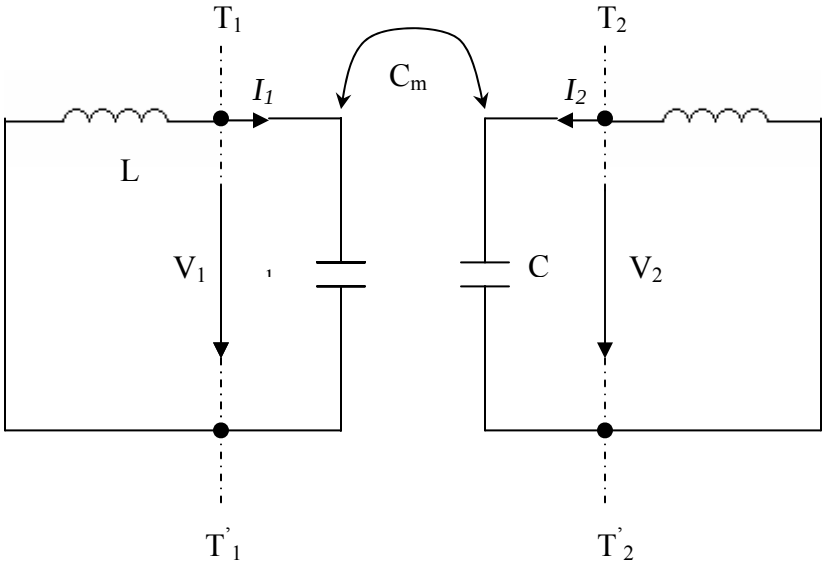

Figure 6.2: Equivalent circuit diagram of the coupled open-loop resonator exhibiting electric coupling

The C and L are the self capacitance and self inductance of the uncoupled resonator and C_m represents the mutual capacitance. The angular resonant frequency of the uncoupled resonator is given by $\frac{1}{\sqrt{LC}}$.

If the network from reference plane T_1-T'_1 to T_2-T'_2 is considered, then we can see a two port network. The following equations describe the network

$$I_1 = j\omega C V_1 - j\omega C_m V_2$$

$$I_2 = j\omega C V_2 - j\omega C_m V_1$$

The second term in the equations corresponds to the current induced by the adjacent resonator. Thus the Y parameters of the network can be given as

$$\begin{bmatrix} Y_{11} & Y_{12} \\ Y_{21} & Y_{22} \end{bmatrix} = \begin{bmatrix} j\omega C & -j\omega C_m \\ -j\omega C_m & j\omega C \end{bmatrix}$$

Alternative form of the network can be drawn with an admittance inverter $J = \omega C_m$ in between the two resonant networks. The resulting equivalent network is shown in the figure.

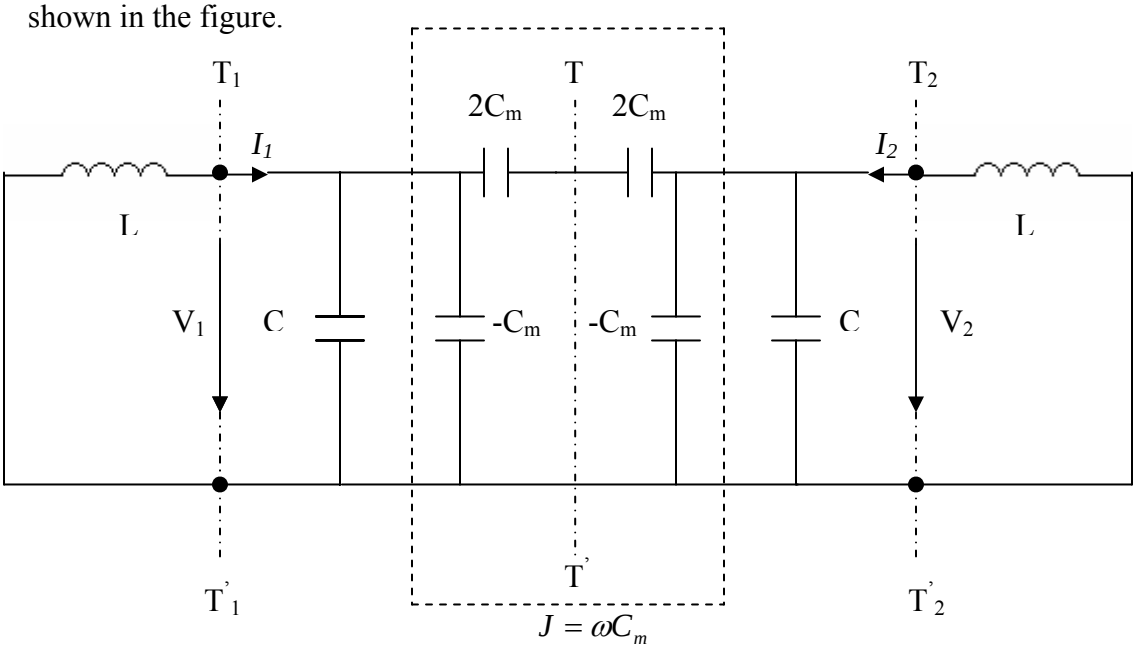

Figure 6.3: Equivalent circuit with admittance inverter $J = \omega C_m$ to represent the coupling

If this equivalent circuit is short circuit at the plane of symmetry T-T', i.e. an electric wall is introduced at the plane T-T', then due to the effect of the adjacent resonator the capability of storing charge of the single resonator is enhanced. This results in a resonant frequency lower than that of the uncoupled resonator.

$$f_e = \frac{1}{2\pi\sqrt{L(C + C_m)}}$$

Similarly when a magnetic wall, i.e. a open circuit, inserted at the plane of symmetry T-T', the coupling effect reduces the capability of storing charge. This results in the increased resonant frequency.

$$f_m = \frac{1}{2\pi\sqrt{L(C - C_m)}}$$

The electric coupling coefficient k_e for the resonant network in terms of the magnetic and electric resonant frequency can be given as

$$k_e = \frac{f_m^2 - f_e^2}{f_m^2 + f_e^2} = \frac{C_m}{C}$$

6.3 Magnetic Coupling

As stated earlier that at resonance the fringe field at the open end is the strongest which results in maximum electric field density at the side with an open gap. The fringe field exhibits an exponentially decaying character outside the region, thus the opposite side to the open end has the maximum fringe field resulting into maximum magnetic field distribution. Thus to achieve magnetic coupling the sides with maximum magnetic field are proximately placed.

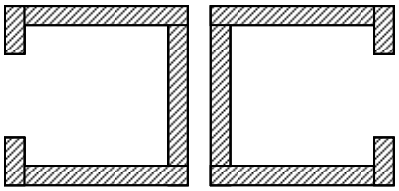

Figure 6.4: Magnetic Coupling Structure

The equivalent circuit of the planar structure can be drawn as

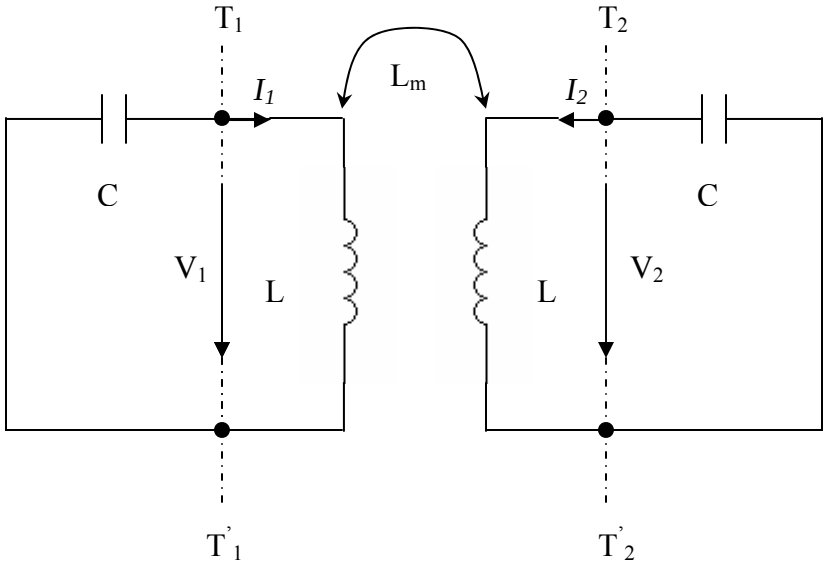

Figure 6.5: Equivalent circuit diagram of the coupled open-loop resonator exhibiting magnetic coupling.

The C and L are the self capacitance and self inductance of the uncoupled resonator and L_m represents the mutual capacitance. The angular resonant frequency of the uncoupled resonator is given by $\frac{1}{\sqrt{LC}}$.

Similarly for this network we can see a two port network. The following equations describe the network

$$V_1 = j\omega L I_1 + j\omega L_m I_2$$

$$V_2 = j\omega L I_2 + j\omega L_m I_1$$

The second term in the equations corresponds to the voltage induced by the adjacent resonator. Thus the Z parameters of the network can be given as

$$\begin{bmatrix} Z_{11} & Z_{12} \\ Z_{21} & Z_{22} \end{bmatrix} = \begin{bmatrix} j\omega L & j\omega L_m \\ j\omega L_m & j\omega L \end{bmatrix}$$

Alternative form of the network can be drawn with an impedance inverter $K = \omega L_m$ in between the two resonant networks. The resulting equivalent network is shown in the figure.

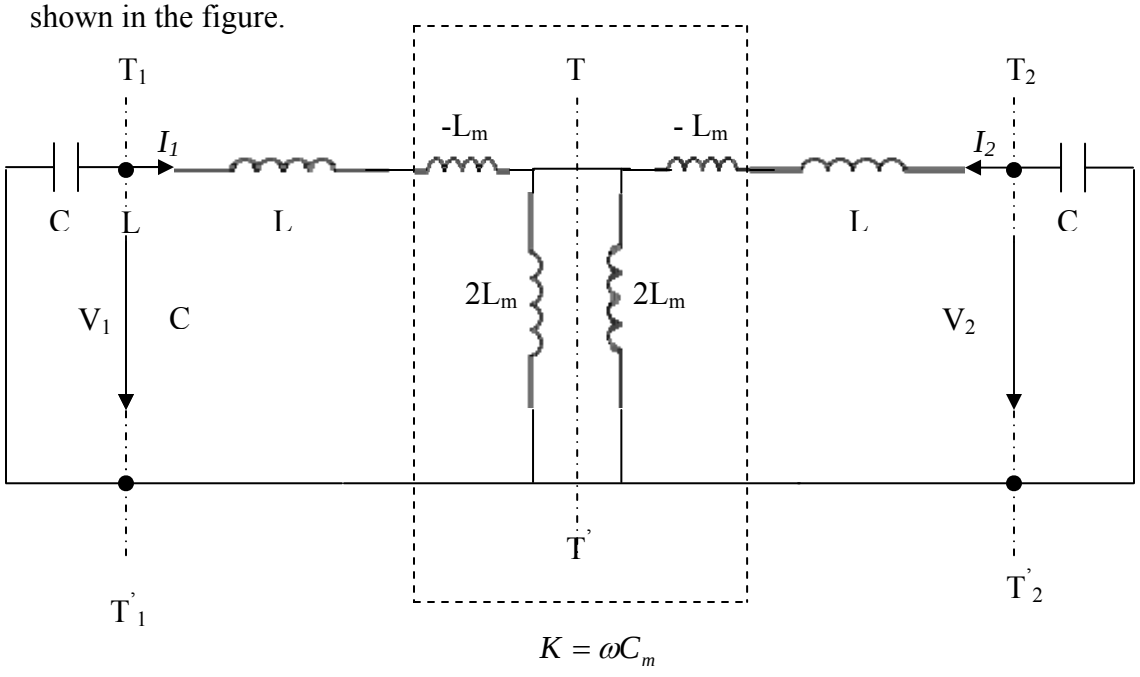

Figure 6.6: Equivalent circuit with impedance inverter $K = \omega L_m$ to represent the coupling

If an electric wall is introduced at the plane T-T', then due to the effect of the adjacent resonator the flux in single resonator is reduced. This results in a resonant frequency higher than that of the uncoupled resonator.

$$f_e = \frac{1}{2\pi\sqrt{(L - L_m)C}}$$

Similarly when a magnetic wall is inserted at the plane of symmetry T-T', the coupling effect increases the stored flux. This results in the resonant frequency lower than that of uncoupled resonator.

$$f_m = \frac{1}{2\pi\sqrt{(L + L_m)C}}$$

The magnetic coupling coefficient k_m for the resonant network in terms of the magnetic and electric resonant frequency can be given as

$$k_m = \frac{f_e^2 - f_m^2}{f_e^2 + f_m^2} = \frac{L_m}{L}$$

6.4 Mixed Coupling

Cases when the electric and magnetic field distribution of the coupled resonator arms are comparable then neither the magnetic coupling nor the electric coupling can be ignored. This type of coupling is called as Mixed Coupling. The following planar structure exhibit Mixed Coupling.

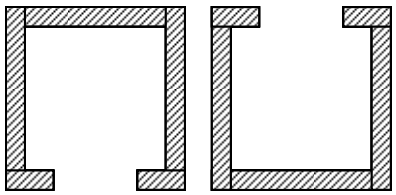

Figure 6.7: Mixed Coupling Structure

This planar structure can be redrawn with impedance and admittance network parameter.

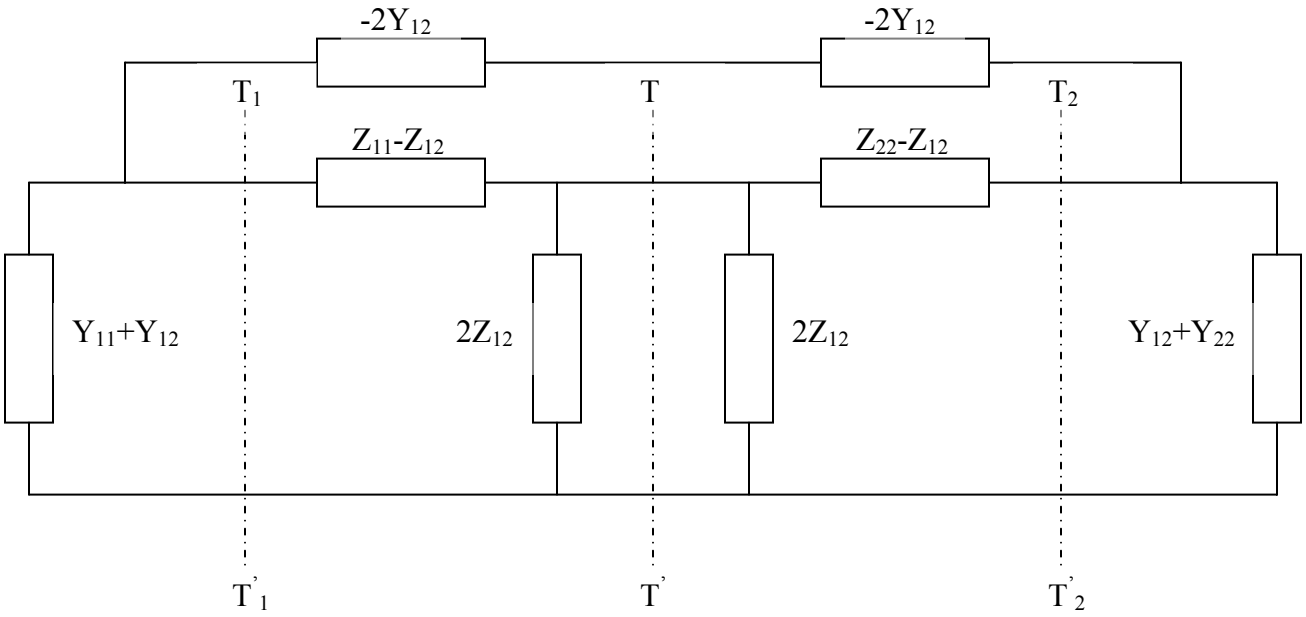

Figure 6.8: Network representation of the open loop resonators exhibiting mixed coupling

The Y network Parameter can be given as

$$\begin{bmatrix} Y_{11} & Y_{12} \\ Y_{21} & Y_{22} \end{bmatrix} = \begin{bmatrix} j\omega C & j\omega C_m^{'} \\ j\omega C_m^{'} & j\omega C \end{bmatrix}$$

And the Z parameter can be given as

$$\begin{bmatrix} Z_{11} & Z_{12} \\ Z_{21} & Z_{22} \end{bmatrix} = \begin{bmatrix} j\omega L & j\omega L_m^{'} \\ j\omega L_m^{'} & j\omega L \end{bmatrix}$$

Where L and C are the self inductance and self capacitance of the individual resonators. And $L_m^{'}$ and $C_m^{'}$ are the mutual inductance and mutual capacitance.
The network can also be drawn using the impedance inverter $K = \omega L_m^{'}$ and admittance inverter $J = \omega C_m^{'}$, which represent magnetic coupling and the electric coupling. Figure6.9 is the equivalent circuit.

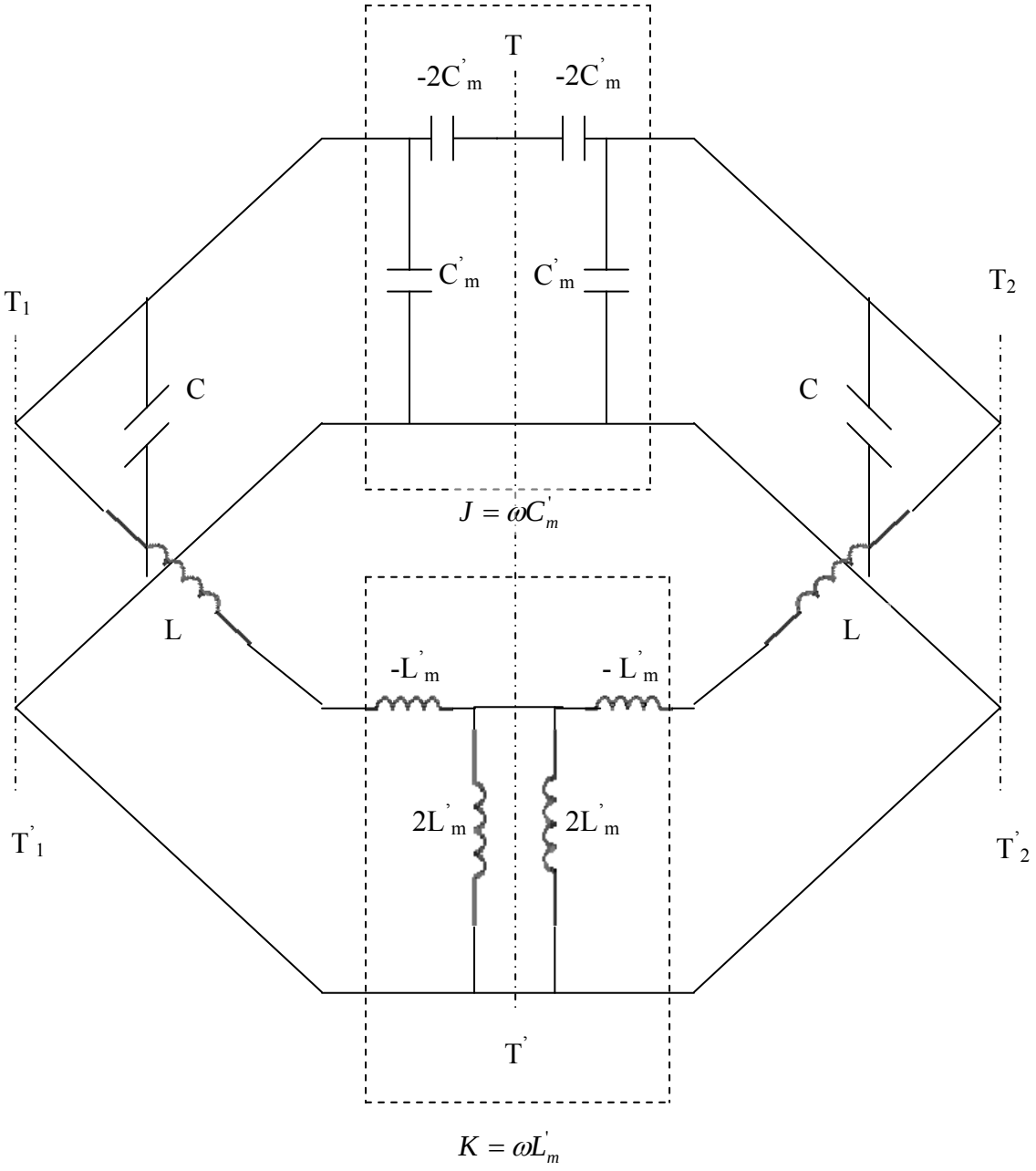

Figure 6.9: Equivalent circuit of mixed coupling with an impedance inverter $k = \omega L_m^{'}$ and an admittance inverter $J = \omega C_m^{'}$ representing the magnetic and electric coupling respectively.

Again by introducing an electric wall and a magnetic wall at the plane of symmetry T-T' one can obtain the electric and magnetic resonant frequency.

$$f_e = \frac{1}{2\pi\sqrt{\left(L - L_m^{'}\right)\left(C - C_m^{'}\right)}}$$

$$f_m = \frac{1}{2\pi\sqrt{\left(L + L_m^{'}\right)\left(C + C_m^{'}\right)}}$$

So the resulting mixed coupling coefficient can be given by

$$k_B = \frac{f_e^2 - f_m^2}{f_e^2 + f_m^2}$$

$$= \frac{CL_m^{'} + LC_m^{'}}{LC + L_m^{'}C_m^{'}}$$

When $L_m^{'}C_m^{'} << LC$ is assumed the above equation yields to

$$k_B \approx \frac{L_m^{'}}{L} + \frac{C_m^{'}}{C}$$

$$= k_M^{'} + k_E^{'}$$

6.5 Coupling Coefficient Graph

For a designer while designing a filter the required dimensions for a particular coupling coefficient is needed. Thus a curve of coupling coefficient versus the coupling spacing with other dimensions of the resonator fixed is used. An EM simulator can be used to obtain the design curve.The following figure shows an EM simulation of the pair of hairpin resonator shown in the figure

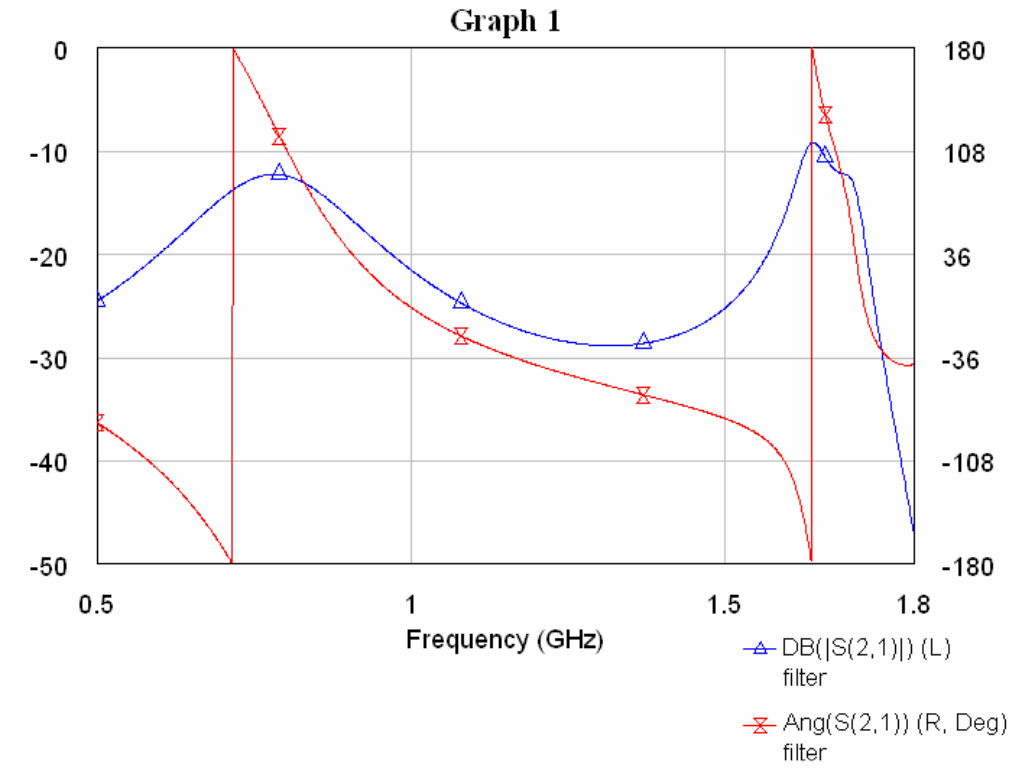

Figure 6.10: Resonant mode splitting phenomenon of the Hairpin Resonator

In the simulated plot one can see two peaks. These correspond to the electric and the magnetic resonance for the resonator and the corresponding coupling coefficient can be calculated. By varying the coupling space with the tuner, various values of resonant frequency can be taken and the respective coupling coefficient can be calculated. These are then plotted on a graph to obtain the coupling coefficient curve.

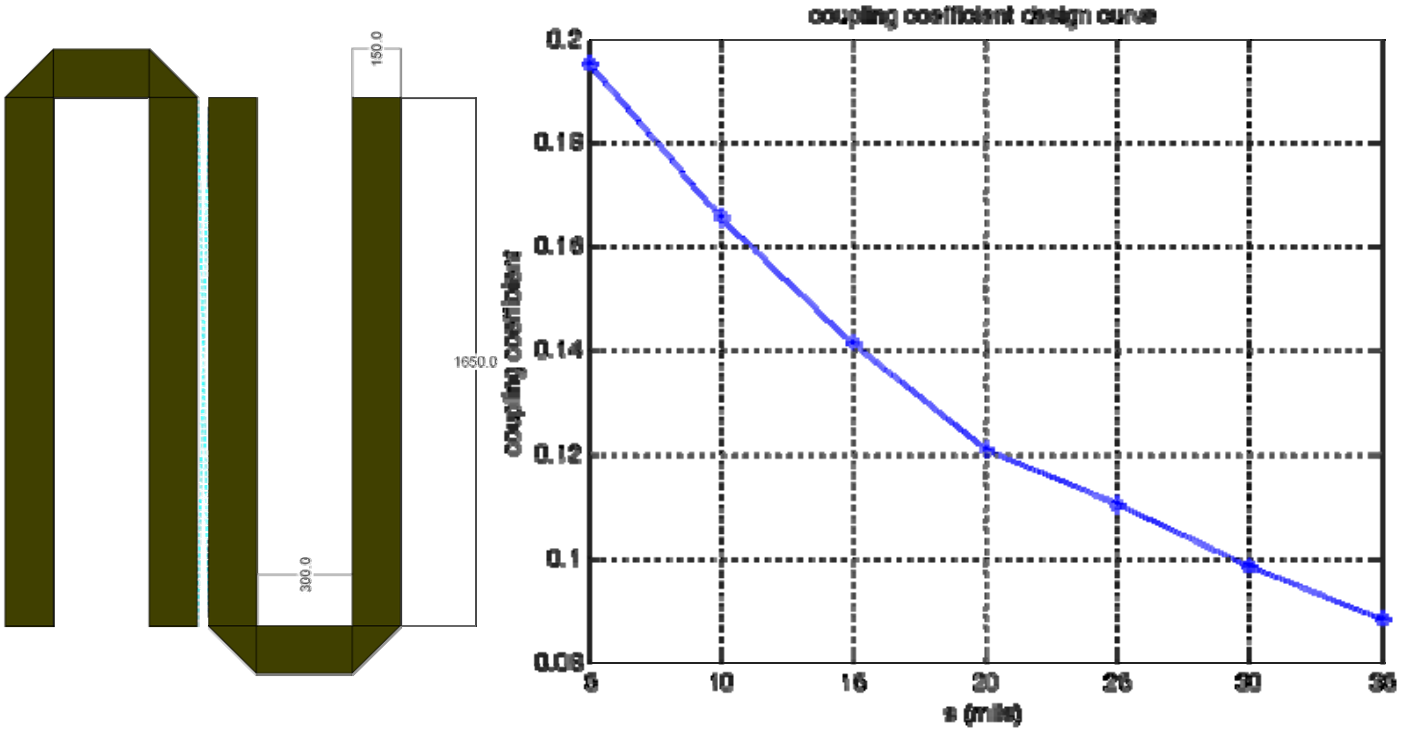

(a) (b)

Figure 6.11: (a) Pair of Hairpin Resonator (b) Coupling Coefficient Curve.

Chapter Seven

Filter Design Using Software

Today's Microwave Engineer rely on advanced simulation software's and electromagnetic analysis tools to develop and analyze microwave circuits. Using these emulators benefit the designer by saving the time for repeated design and testing phase and give the good approximation of the expected results.

For the design of the bandpass filter, the design procedure using the AWR Microwave Office simulation program developed by Applied Wave Research USA will be described in this section.

7.1 Schematic of Filter

The individual hairpin resonators can be modeled using the numerical models deveoped by AWR.

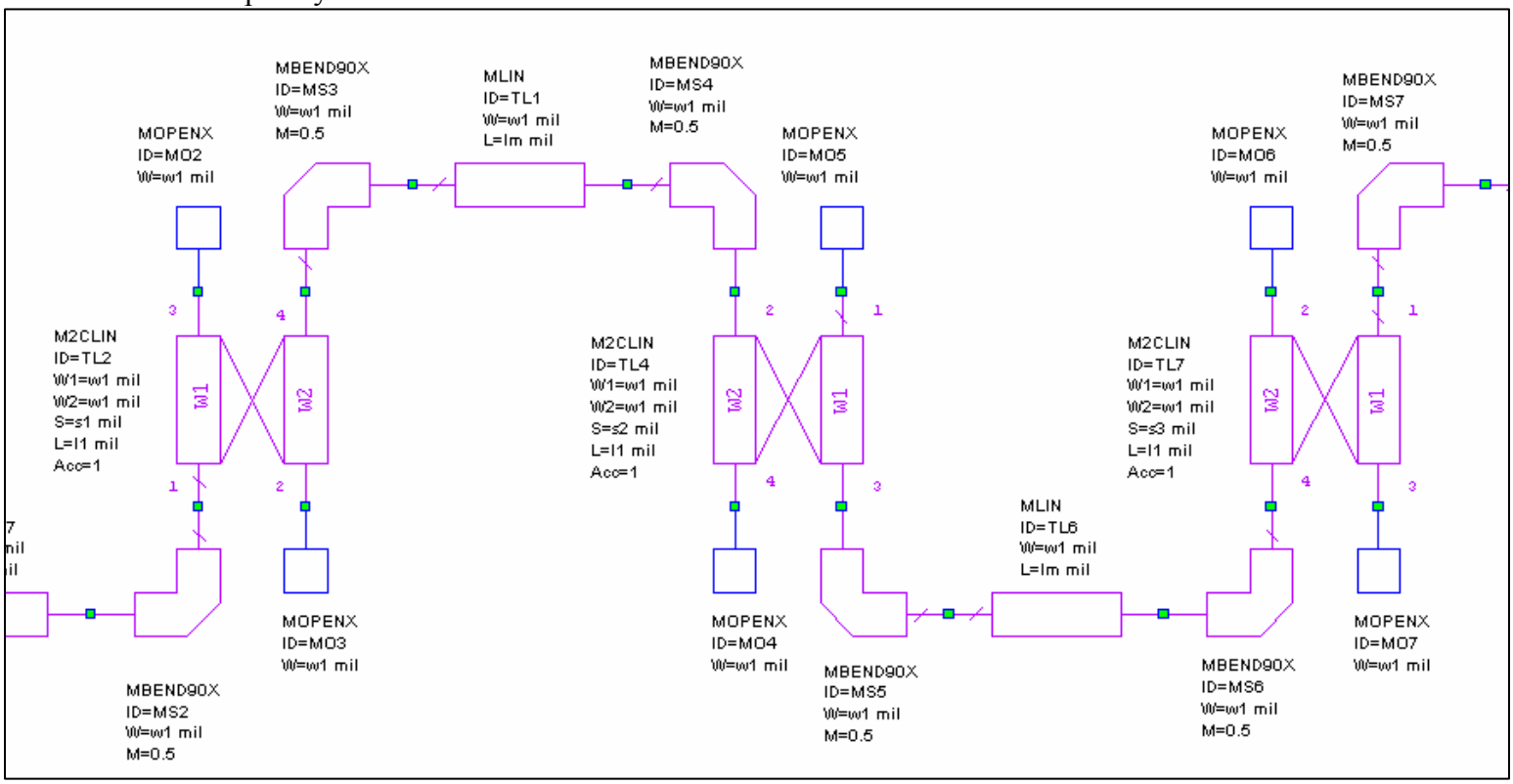

Figure 7.1: Section of Schematic in AWR Microwave Office

The mopen(Open Circuit With End Effect (Closed Form)) model takes into account the fringing effect of the conductor. The mline element models a length of Microstrip Transmission Line. The model assumes a Quasi-TEM mode of propagation and incorporates the effects of dielectric and conductive losses. M2clin is advanced numerical model representing two edge coupled line. The distance between the bends of an individual resonator is kept more than twice the width of the microstrip conductor.

To calculate the approx length of each hairpin resonator the TXline calculator of MWO is used.

The dielectric used for this design is FR4. Its specifications are:

Substrate thickness: 1.6mm

Relative dielectric constant: 4.4

Conductor: copper

Conductor thickness: 35µm

Loss tangent: 0.022

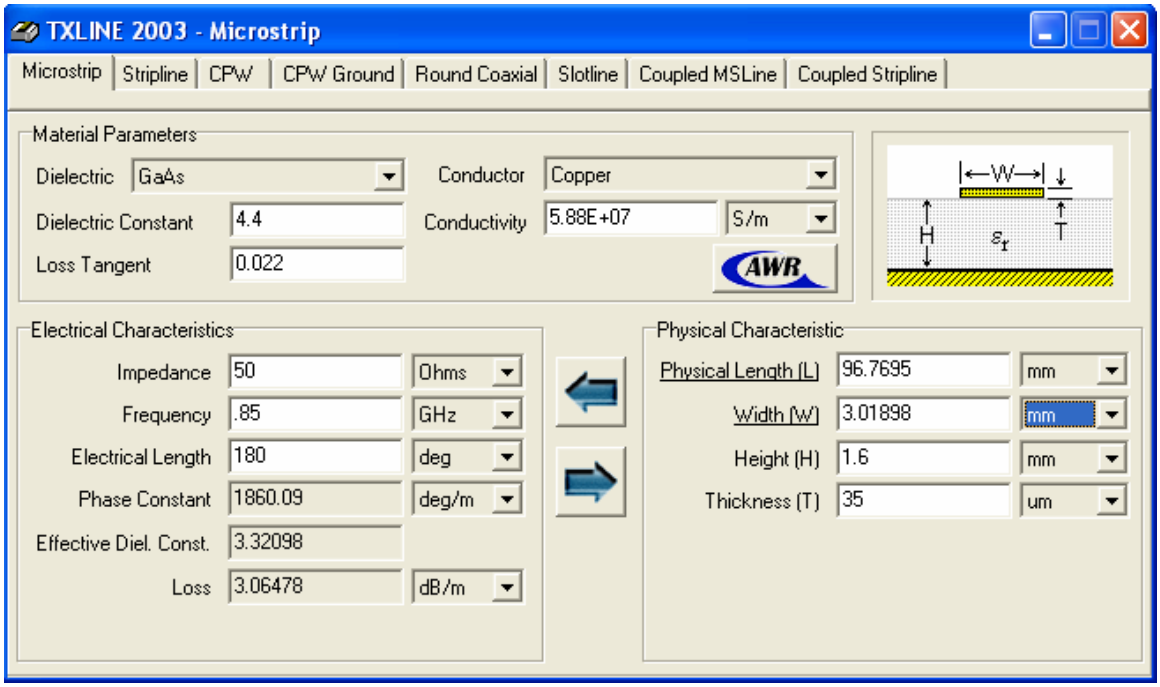

Figure 7.2: TXLINE Calculator of AWR Microwave Office

7.2 800-900 MHz Bandpass Filter Design

I: Hairpin Filter Specification

- Passband 800-900MHz
- 7 Pole Filter
- 25dB rejection at 920MHz
- 25dB rejection at 780MHz
- Return Loss>12dB
- Substrate Material FR4

II: Open Loop, Cross coupled Filter

- Passband 800-900MHz
- 4 Pole Filter
- 25dB rejection at 920MHz
- 25dB rejection at 780MHz
- Return Loss>12dB
- Substrate Material FR4

7.3 Design Procedure

First the length of the resonators for the center frequency 850 MHz is calculated using the TXline calculator of "Microwave Office by AWR". Then the schematic of the design is created. In the schematic the length of each resonator is summed up to the length calculated by the TXline calculator. MSUB substrate is added to the schematic and the values are set to the specification of FR4 substrate. A graph is added to the schematic with measurement S_{21} and S_{11}. Next various dimensions of the schematic are made variable and they are tuned to obtain an approximate pass band at 850 MHz.

Then various optimization goals are set according to the requirement of the design. After the optimization if the requirements are met then the design is finalized or else it is tuned and optimized again till the desired results are obtained.

7.4 Schematics

7.4.1 Hairpin Filter

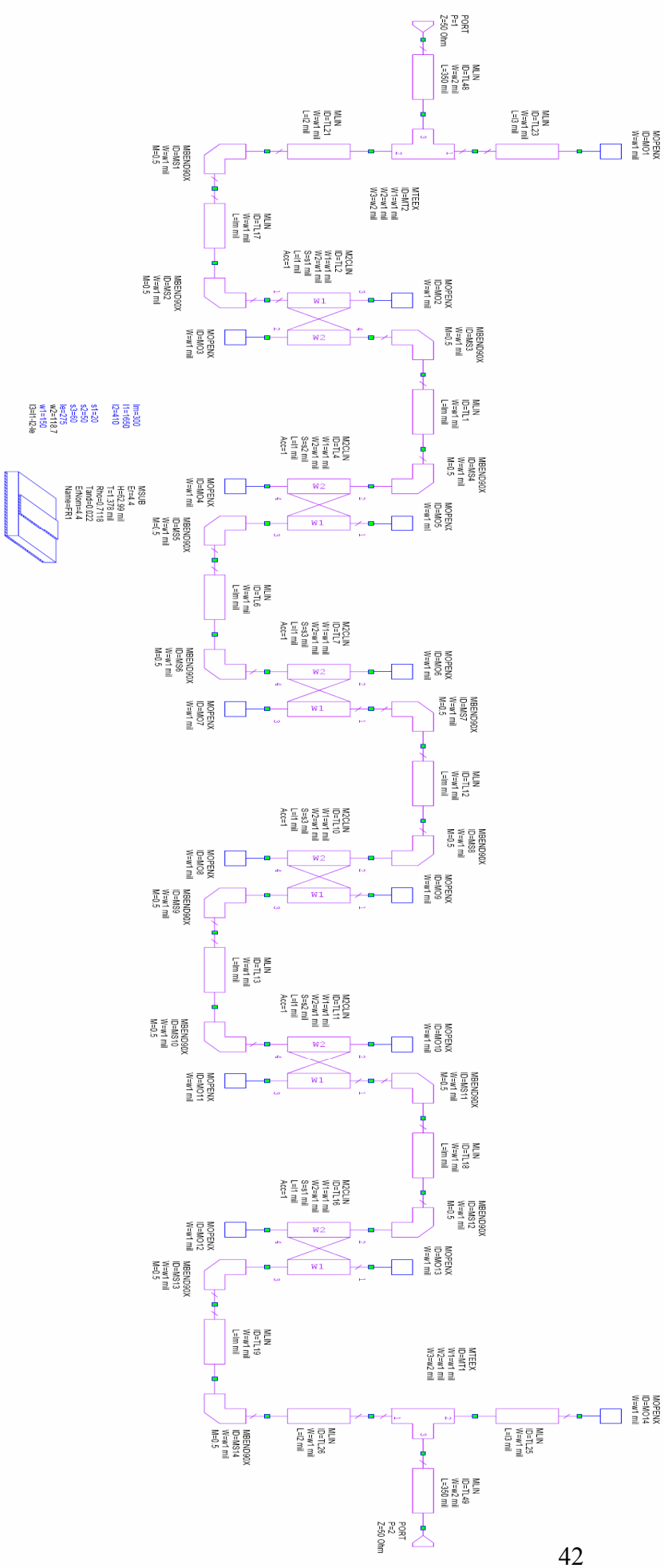

Figure 7.3: Schematic of Hairpin Filter Using AWR Microwave Office

7.4.2 Open Loop, Cross Coupled Filter

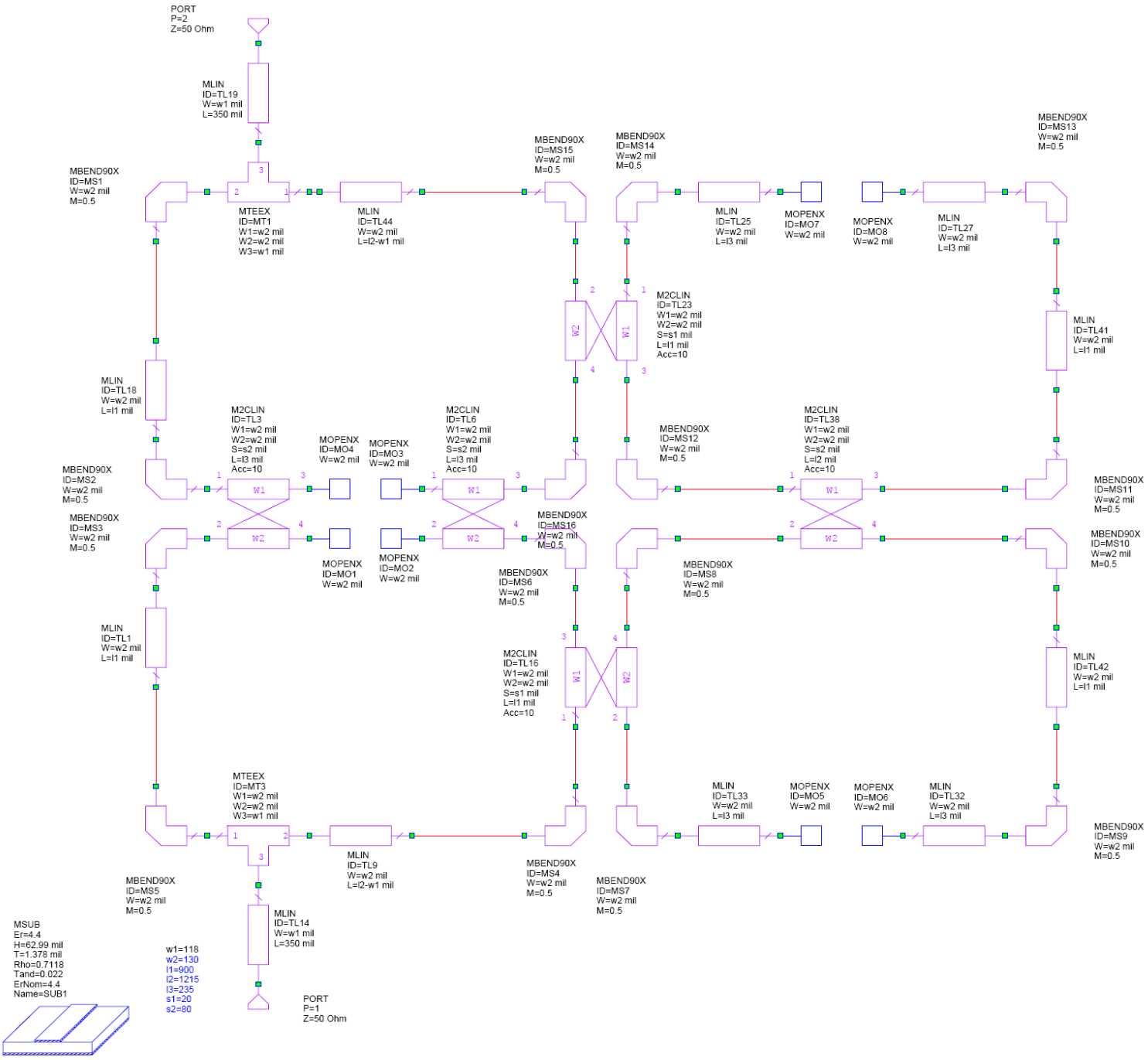

Figure 7.4: Schematic of Open Loop, Cross coupled Filter Using AWR Microwave Office

7.5 Simulated Response

7.5.1 Hairpin Filter

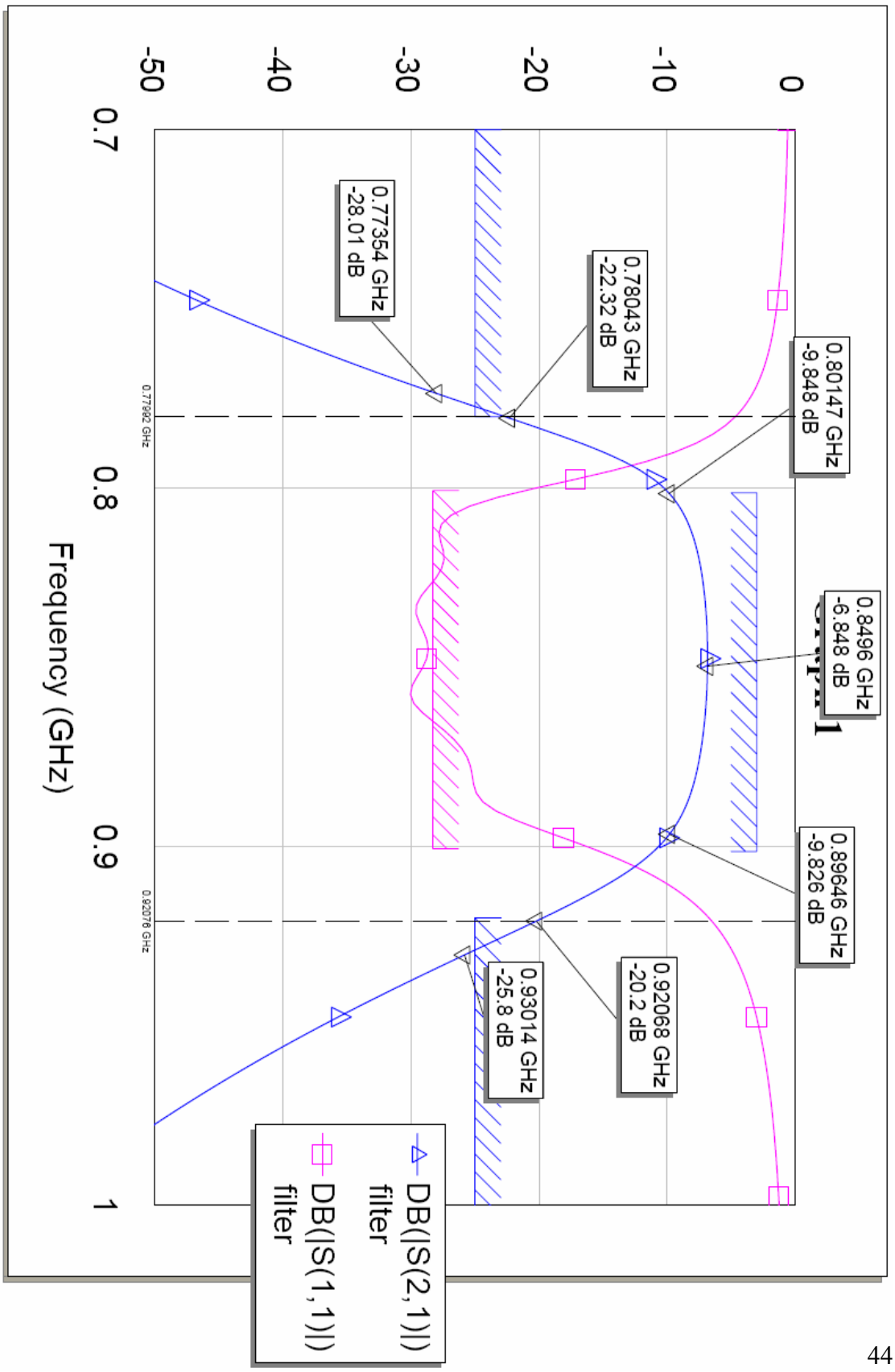

Figure 7.5: Simulated Response of Hairpin Filter Using AWR Microwave Office

7.5.2 Open Loop, Cross Coupled Filter

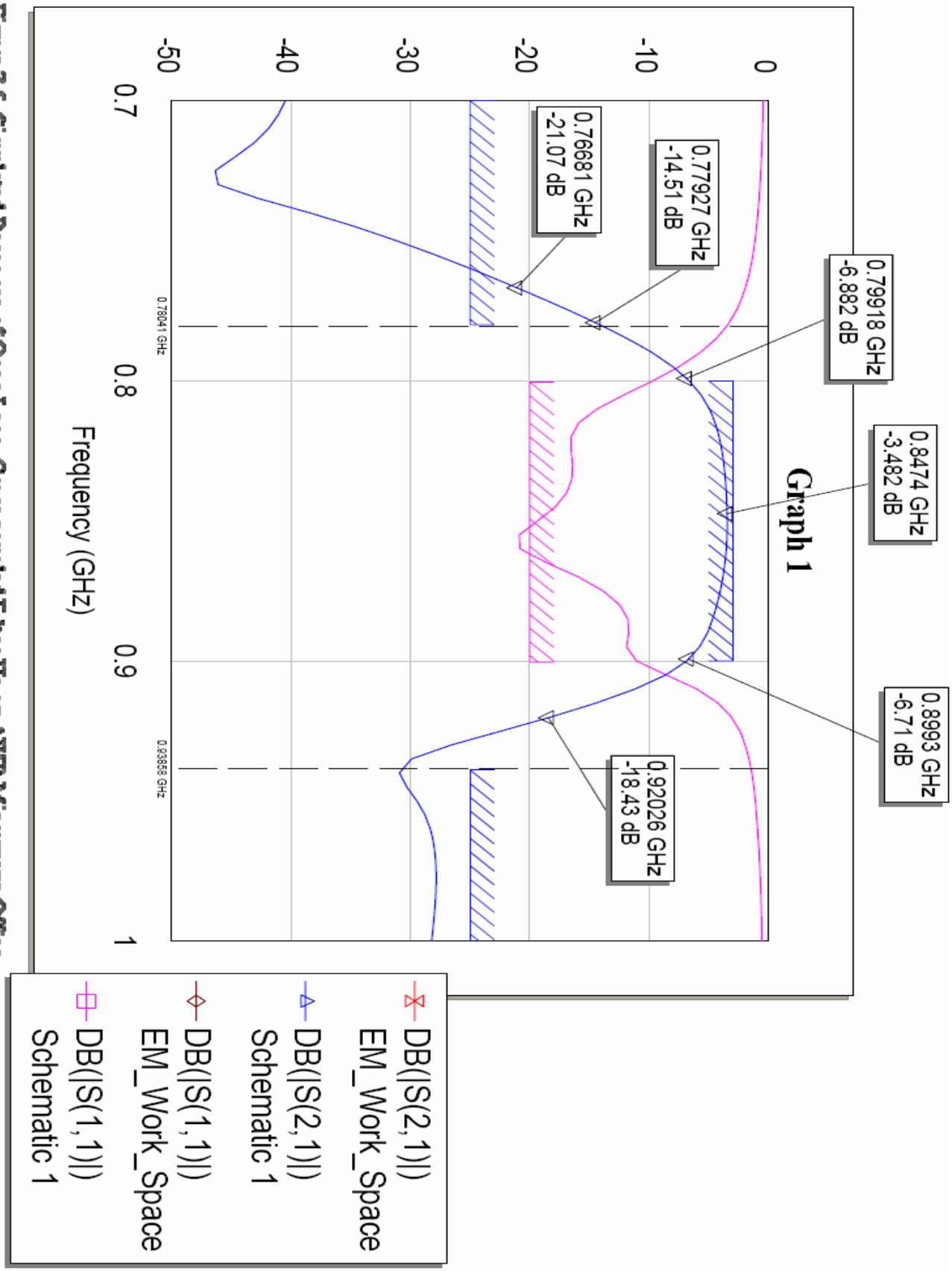

Figure 7.6: Simulated Response of Open Loop, Cross coupled Filter Using AWR Microwave Office

Chapter Eight
Results

Hairpin Band Pass filter

Figure 8.1: Photograph of the Designed Hairpin Filter.

Open Loop, Cross Coupled Filter

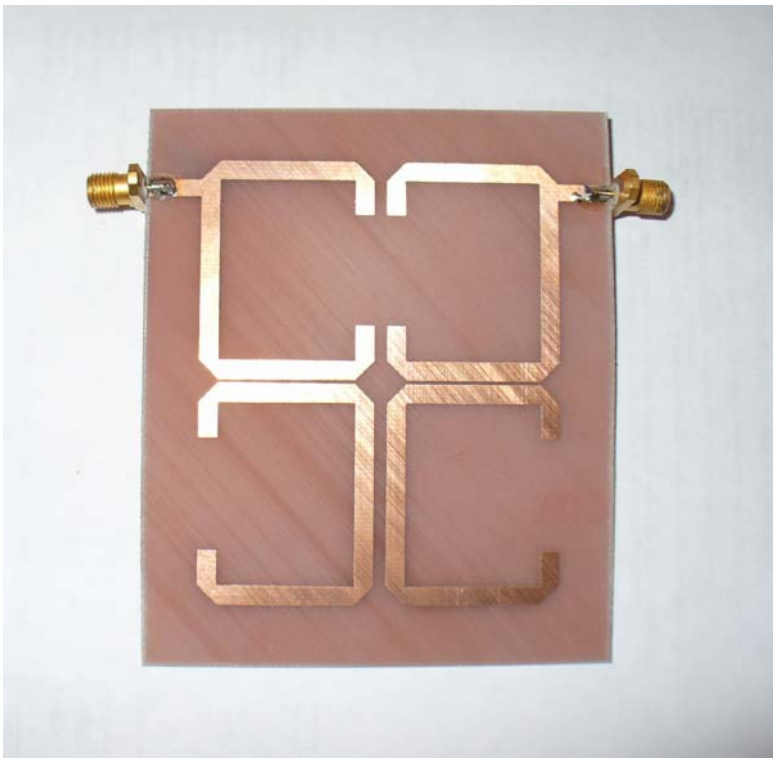

Figure 8.2: Photograph of the Designed Open Loop, Cross coupled Filter.

8.1 Layout

8.1.1 Hairpin Filter

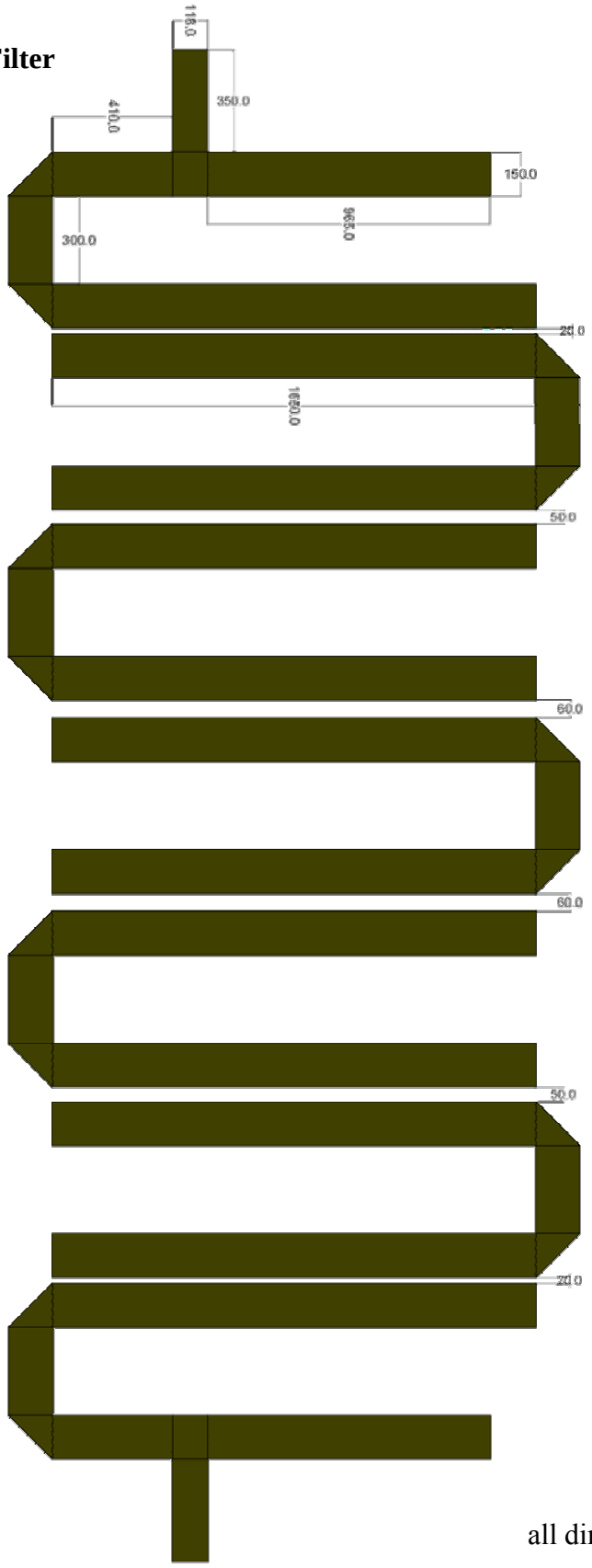

all dimensions in mils

Figure 8.3: Dimensional Layout of Hairpin Filter.

8.1.2 Open Loop, Cross Coupled Filter

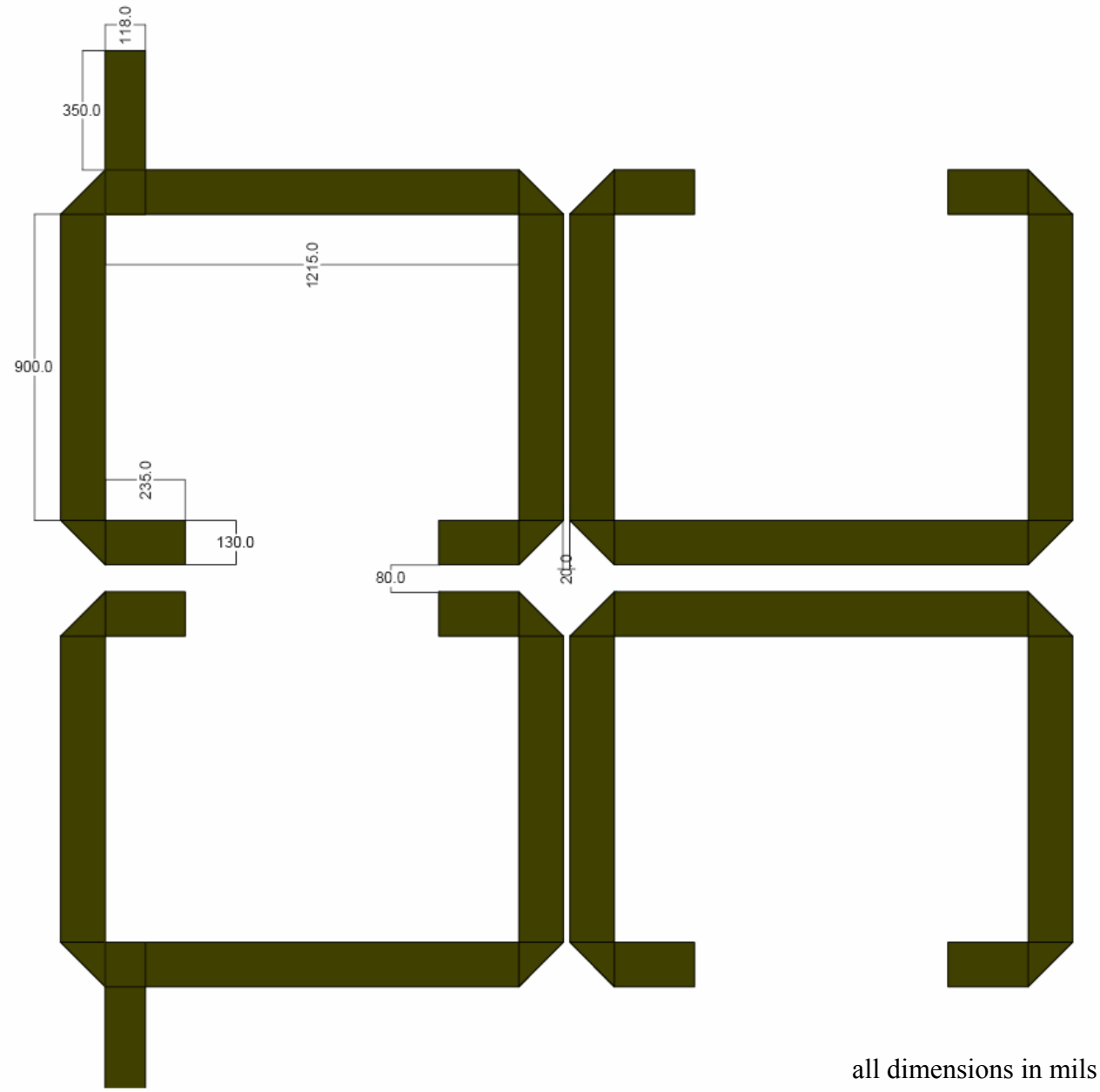

Figure 8.4: Dimensional Layout of Open Loop, Cross coupled Filter.

8.2 Measured Response

8.2.1 Hairpin Filter

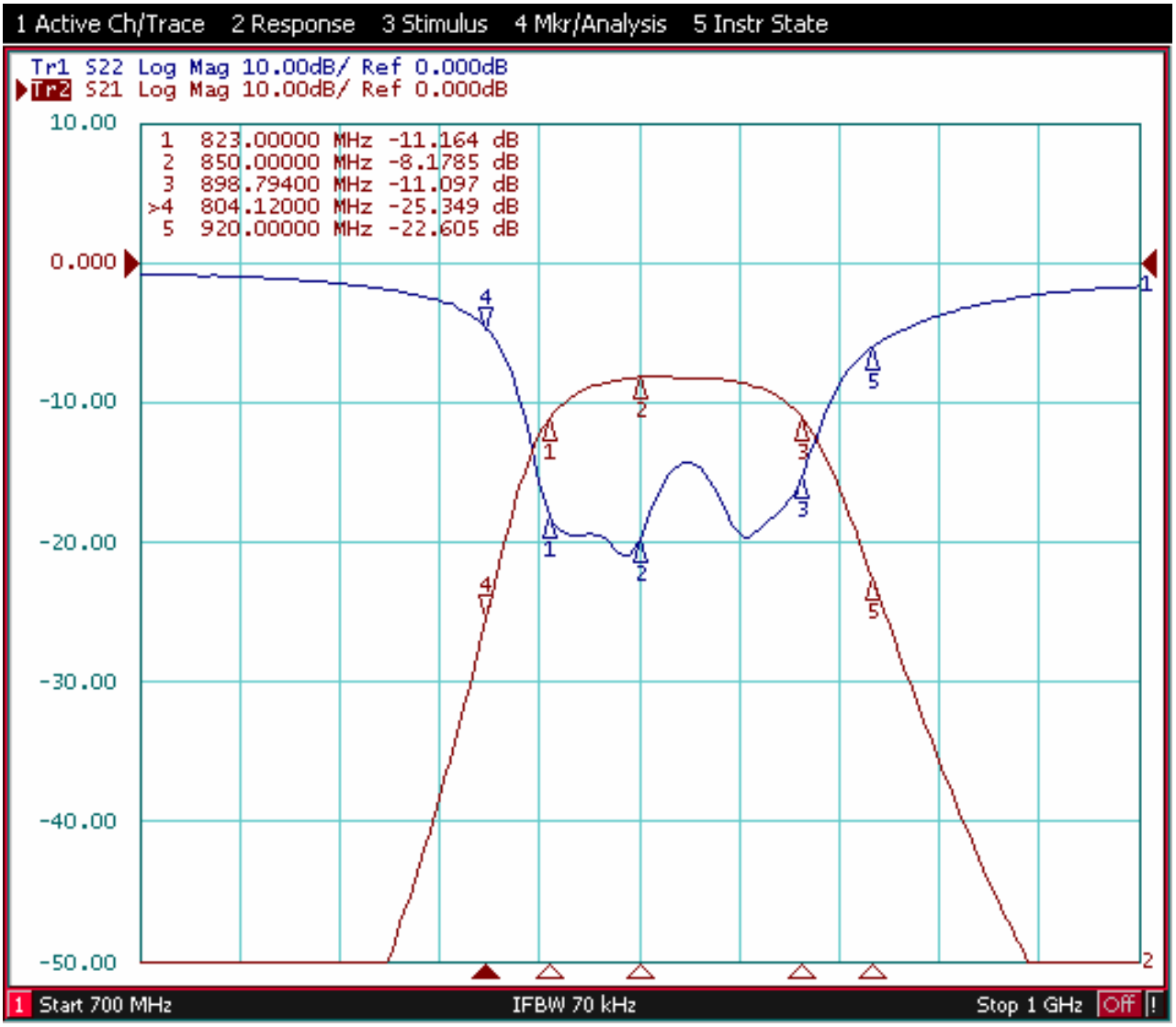

Figure 8.5: Network Analyzer Plot for Hairpin Filter.

8.2.2 Open Loop, Cross Coupled Filter

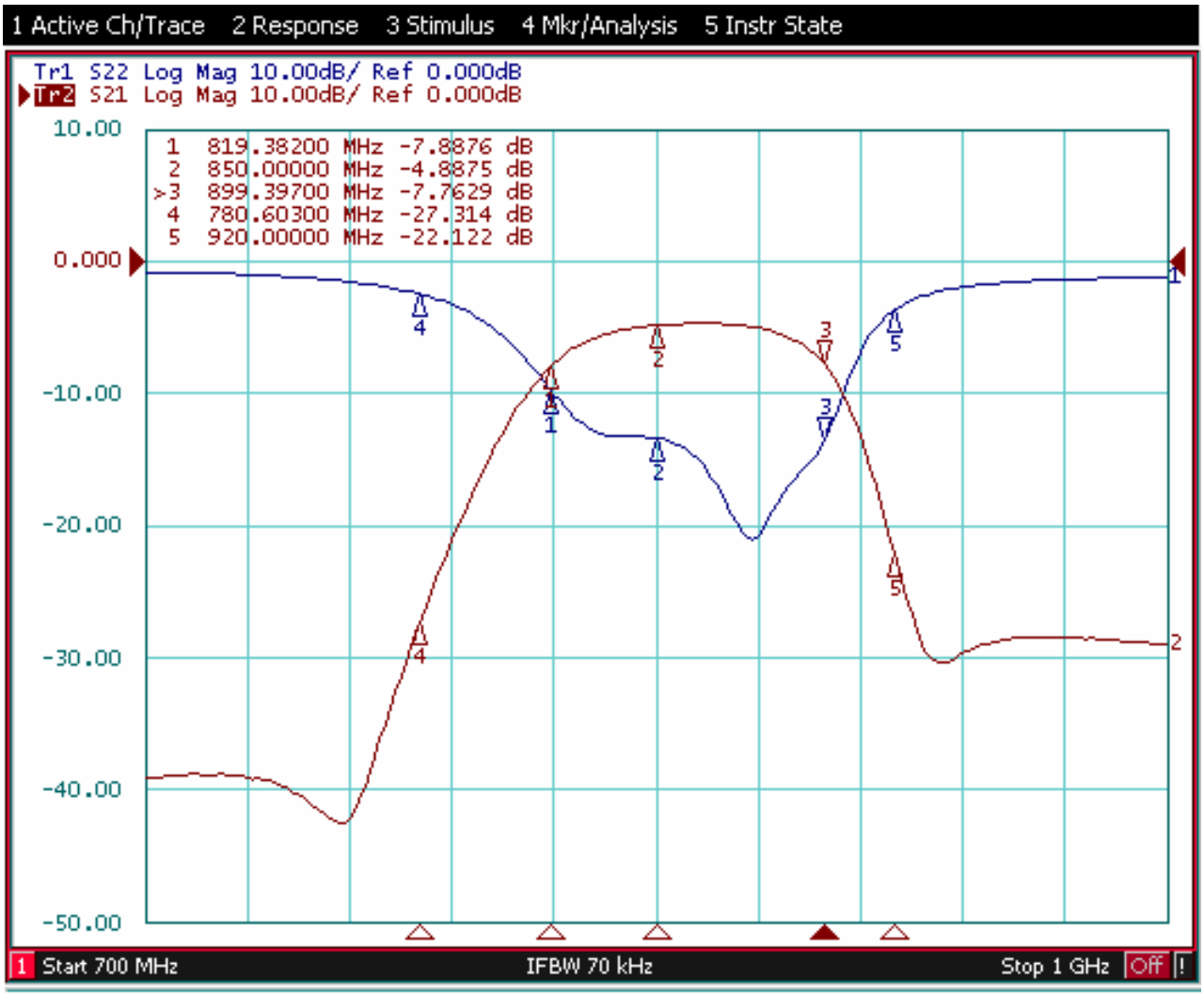

Figure 8.6: Network Analyzer Plot for Open Loop, Cross coupled Filter.

8.3 Comparison Table

Parameters	Hairpin Filter	Open Loop, Cross Coupled Filter
Start Frequency	823 MHz	819 MHz
Stop Frequency	898 MHz	899 MHz
Bandwidth	75 MHz	80 MHz
Insertion Loss(850MHz)	8.7 dB	4.8 dB
Return Loss(850MHz)	14.8 dB	14.5 dB
Insertion Loss(700MHz)	70 dB	38 dB
Insertion Loss(1GHz)	64 dB	28 dB

Table 8.1: Comparison Between Hairpin And Open Loop, Cross Coupled Filters

References

[1] J. S. Wong, "Microstrip tapped-line filter design," *IEEE Trans. Microwave Theory Tech.,* vol. MTT-27, pp. 44-50, Jan. 1979.

[2] J. S. Hong and M. J. Lancaster, "Canonical microstrip filter using square open-loop resonators," *Elec. Lett.,* vol. 31, pp. 2020-2022, 1995.

[3] R. Levy, "Filters with single transmission zeros at real or imaginary frequencies," *IEEE Trans. Microwave Theory Tech.,* vol. MTT-24, pp.172–181, 1976.

[4] J. S. Hong and M. J. Lancaster, "Couplings of microstrip square open-loop resonators for cross-coupled planar microwave filters," *IEEE Trans. Microwave Theory Tech.,* vol. 44, pp. 2099–2109, 1996.

[5] J. S. Hong and M. J. Lancaster, "Theory and experiment of novel microstrip slow-wave open-loop resonator filters," *IEEE Trans. Microwave Theory Tech.,* vol. 45, pp. 2358–2365, 1997.

[6] "Investigation of novel microwave surface-acoustic-wave filter on different piezoelectric substrates," *Japanese Journal of Applied Physics*, Vol. 43, No. 12, 2004, pp. 8139–8145

[7] Dana Brady (CAP Wireless, Inc), "The Design, Fabrication and Measurement of Microstrip Filter and Coupler Circuits," From July 2002 *High Frequency Electronics,* Summit Technical Media, LLC.

[8] Michael A. Imparato, Ryan C. Groulx and Raphael Matarazzo (Aeronix, Inc), "Design of a Microstrip Bandpass Filter Using Advanced Numerical Models," From March 2004 *High Frequency Electronics,* Summit Technical Media, LLC.

[9] Kamaljeet Singh, R. Ramasubramanian, S. Pal Communication Systems Group, ISRO Satellite Center, Bangalore, India, "Coupled Microstrip Filters: Simple Methodologies for Improved Characteristics".

[10] Peter Martin RFshop, "Designing edge-coupled microstrip bandpasss filter using Microwave Office^{TM}".

[11] E. G. Cristal and S. Frankel, "Hairpin-line and hybrid hairpin-line/half-wave parallel-coupled-line filters," *IEEE Trans. Microwave Theory Tech.,* vol. MTT-20, No. 11, pp. 719–728, 1972.

[12] U. H. Gysel, “New theory and design for hairpin-line filters,” *IEEE Trans. Microwave Theory Tech.,* vol. MTT-22, No. 5, pp. 523–531, 1974.

[13] G. L. Matthaei and N. O. Fenzi, “Hairpin-comb filters for HTC and other narrow-band applications,” *IEEE Trans. Microwave Theory Tech.,* vol. 45, pp. 1226–1231, 1997.

[14] E. 0. Hammerstad and 0. Jensen, "Accurate models for microstrip computer-aided design," *IEEE MTT-S,* 1980, Digest, pp. 407409.

[15] Jia-Shen G. Hong and M. J. Lancaster, “Microstrip Filters for RF/Microwave Applications,” Willey Series in Microwave and Optical Engineering.

Appendix A

Filter Basics

Filters play an important role in the RF/Microwave application. They are used to separate various frequencies. Filters are typically two port networks. They rely on impedance mismatching to reject RF energy. Filters are primarily used to confine or select RF/Microwave signals within a specified spectral limit.

The response of a filter can be mathematically expressed in terms of its S_{21} parameter. It is called as the transfer function of the filter. Many a times it is expressed in amplitude squared transfer function of a filter given as:

$$\left|S_{21}(j\omega)\right|^2 = \frac{1}{1+\varepsilon^2 F_n{}^2(\omega)}$$

where ε is a ripple constant and $F_n(\omega)$ represents the filtering characteristics function and ω is the frequency variable in radians.

By conventional definition, the insertion loss can be computed as

$$L_A(\omega) = 10\log\frac{1}{\left|S_{21}(j\omega)\right|^2}\ \text{dB}$$

For a lossless passive two-port network $\left|S_{11}\right|^2 + \left|S_{21}\right|^2 = 1$ from which return loss can be calculated as

$$L_R(\omega) = 10\log\left[1-\left|S_{21}(j\omega)\right|^2\right]\ \text{dB}$$

Phase response and group delay of the filter can be found as

$$\phi_{21} = Arg\ S_{21}(j\omega)$$

$$\tau_d(\omega) = \frac{d\phi_{21}(\omega)}{-d\omega}\ \text{seconds}$$

A.1 Pole zero concept

For linear time invariant networks, transfer function can be given as

$$S_{21}(j\omega) = \frac{N(p)}{D(p)}$$

where p is the complex frequency variable.

$$p = \sigma + j\omega$$

σ is neper frequency and ω is complex frequency variable. The values of p for which the function becomes zero are called zeros of the filter and values for which the function becomes infinite are called poles of the function. These zeros and singularities are important in determining the stability and the response of the filter. These complex frequencies can be represented as symbols on (σ, ω) plane called complex plan. Where the abscissa is the real component of the root and the ordinate is the imaginary part. For the filter to be stable, these natural frequencies should lie on the left of the plan.

A.2 Some Filter Response

A.2.1 Butterworth Response

Butterworth filter response is also known as maximally flat filter response. The amplitude square function of Butterworth filter is given by

$$\left|S_{21}(j\omega)\right|^2 = \frac{1}{1+\omega^{2n}}$$

Where n is the order of the filter and signifies number of independent energy storage elements required in the filter as well as to the power of ω with which the response magnitude rolls off. The attenuation increases steadily with frequency, giving a maximally flat approximation to a low pass filter. The attenuation at the cut off frequency $\omega_c = 1$ is 3.01db.

As the order of the filter increases the roll of becomes sharper. The Butterworth is the only filter that maintains this same shape for higher orders (but with a steeper decline

in the stopband) whereas other varieties of filters (Bessel, Chebyshev, Elliptic) have different shapes at higher orders.

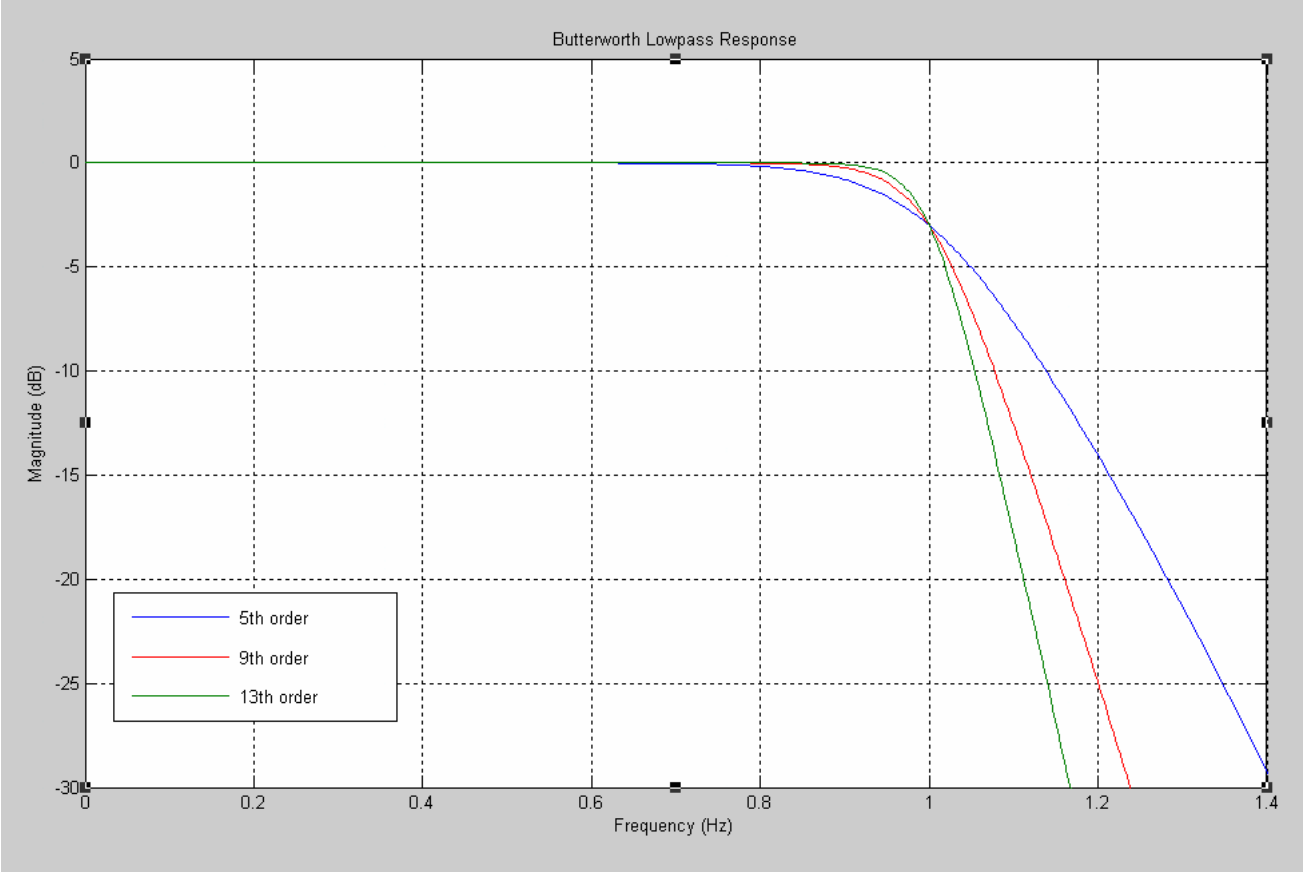

Figure A.1: Butterworth Lowpass Response.

The Butterworth approximation leads to a filter which has moderate attenuation steepness and acceptable characteristics. It provides a better group delay than chebyshev response.

A.2.2 Chebyshev Response

The Chebyshev response is a mathematical strategy for achieving a faster roll off by allowing ripple in the frequency response. Analog and digital filters that use this approach are called Chebyshev filters. Figure A.2 shows the frequency response of low-pass Chebyshev filters with passband ripples of 0dB, 1db, 2db and 4db. As the ripple

increases, the roll-off becomes sharper. The 0dB ripple curve is equivalent to Butterworth response. The Chebyshev response is an optimal trade off between these two parameters.

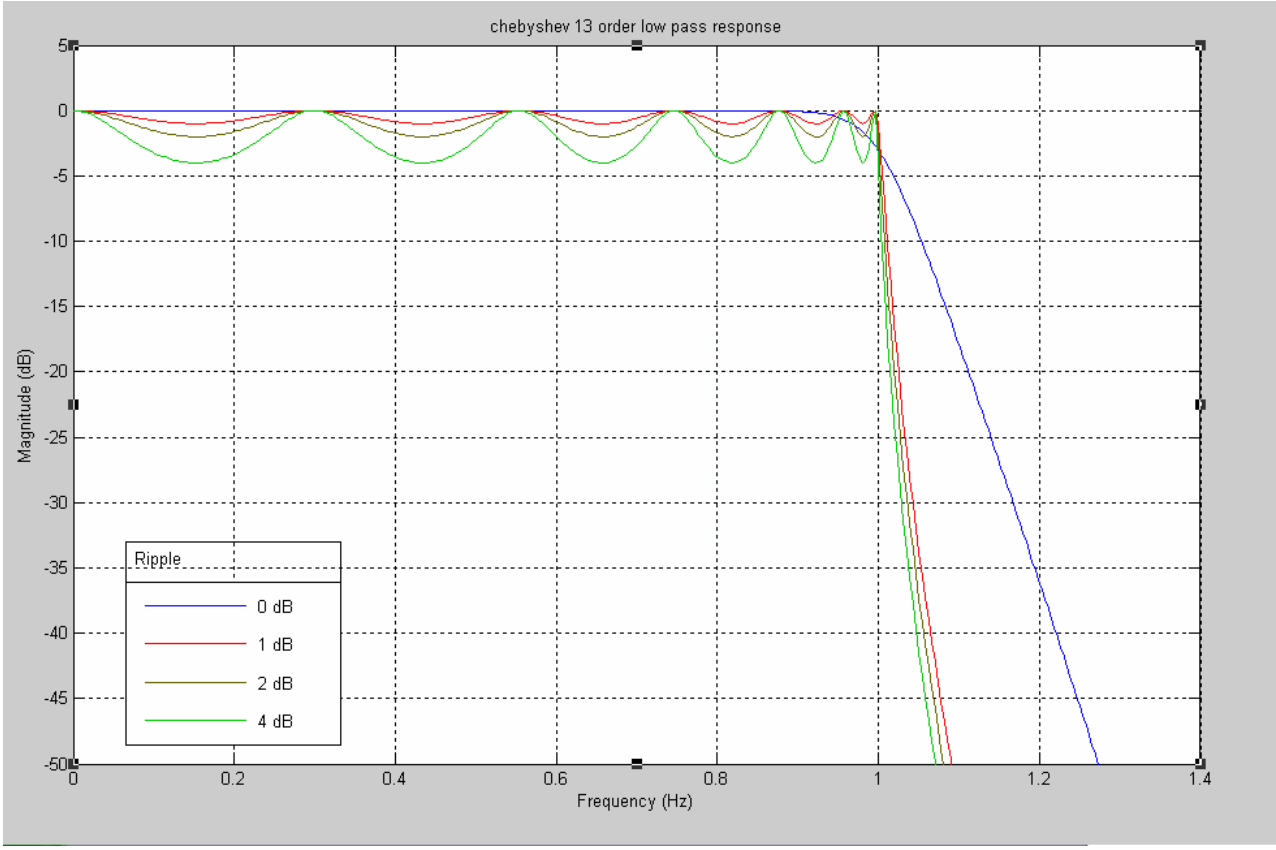

Figure A.2: 13th order Chebyshev Lowpass Response.

The amplitude squared transfer function of the response that describes this type of response is

$$|S_{21}(j\omega)|^2 = \frac{1}{1+\varepsilon^2 T_n^2(\omega)}$$

where the ripple constant is relate to a given pass band ripple L_{AR} in db by

$$\varepsilon = \sqrt{10^{\frac{L_{Ar}}{10}} - 1}$$

$T_n(\omega)$ is a chebyshev function of the first kind of order n, which is defined as

$$T_n(\omega) = \begin{cases} \cos\left(n\cos^{-1}\omega\right) & |\omega| \le 1 \\ \cosh\left(n\cosh^{-1}\omega\right) & |\omega| \ge 1 \end{cases}$$

Similar to the Butterworth filter chebyshev response also have all the zeros at infinity and hence it is also a all pole filter response. On the other hand the arrangement of the poles is different from a Butterworth response. Here the poles lie on an ellipse with major axis on the $j\omega$ axis and its size is $\sqrt{1+\eta^2}$. The minor axis is on σ axis and is of size η.

$$\eta = \sinh\left(\frac{1}{n}\sinh^{-1}\frac{1}{\varepsilon}\right)$$

The slope in the phase response is steepest in the neighborhood of the 3db cut off frequency leading to a group delay peak at cut off frequency.

A.2.3 Elliptical Function Response

As seen earlier in the case of Chebyshev response that allowing ripple in passband or stopband confers desirable transition band. Thus it is not surprising that there will be a further improvement by allowing equi-ripple response in both passband and stopband.

Elliptical filters exploit the nulls provided by finite zeros to create a dramatic transition from passband to stopband at the expense of stopband response that later bounce back some amount beyond the null frequency.

The transfer function of this type of response is given by

$$\left|S_{21}(j\omega)\right|^2 = \frac{1}{1+\varepsilon^2 F_n^2(\omega)}$$

where

$$F_n(\omega) = \begin{cases} M\dfrac{\prod_{i=1}^{n/2}\left(\omega_i^2-\omega^2\right)}{\prod_{i=1}^{n/2}\left(\omega_s^2/\omega_i^2-\omega^2\right)} & \text{for } n \text{ even} \\ N\dfrac{\omega\prod_{i=1}^{(n-1)/2}\left(\omega_i^2-\omega^2\right)}{\prod_{i=1}^{(n-1)/2}\left(\omega_s^2/\omega_i^2-\omega^2\right)} & \text{for } n(\geq 3) \text{ odd} \end{cases}$$

ω_i represent the critical frequencies and ω_s is the frequency at which the equi-ripple stop band starts. M and N are the variables which help specify the minimum in the stopband ripple.

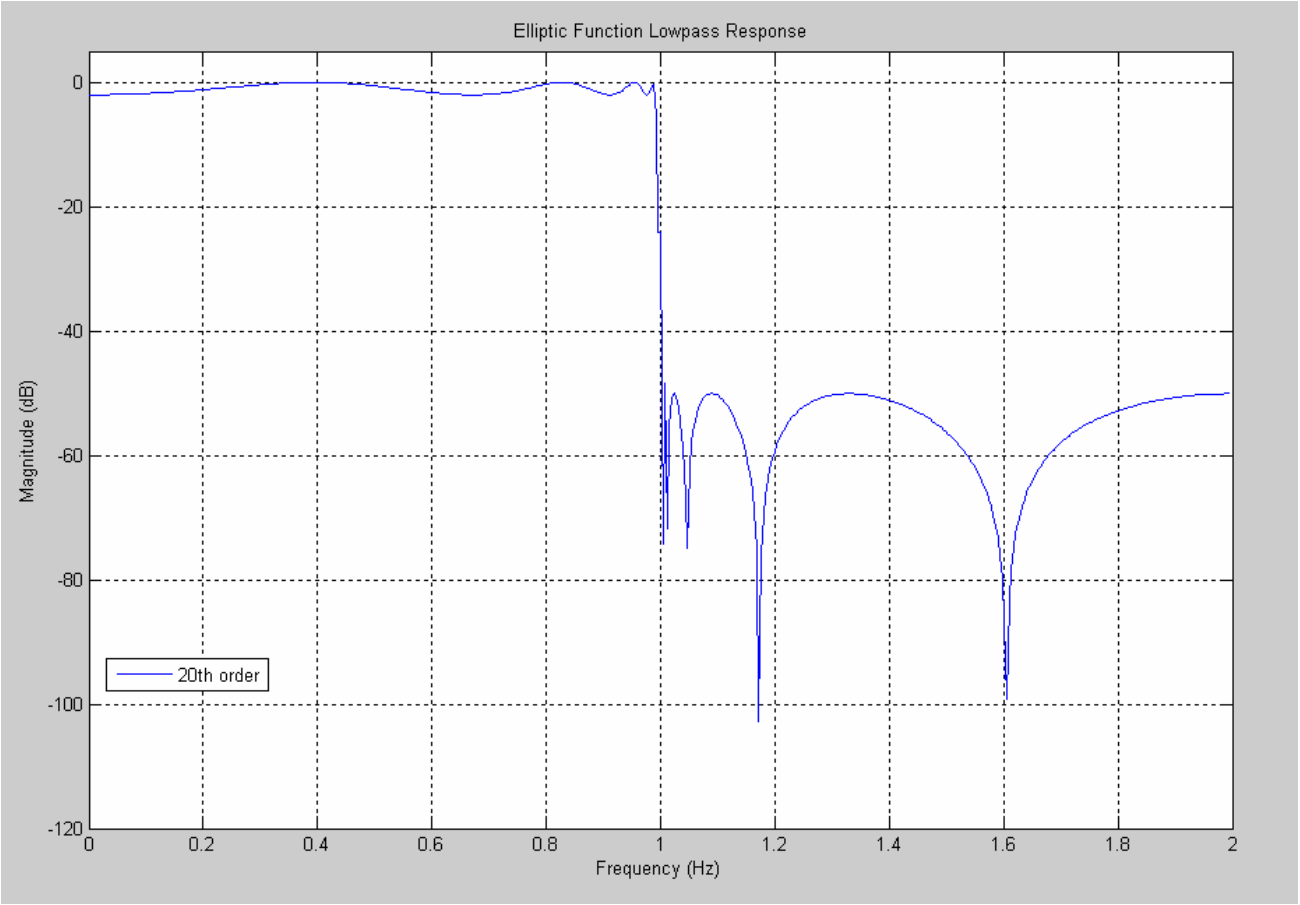

Figure A.3: 20th order Elliptical Function Lowpass Response.

A.2.4 Bessel Filters (Maximally Flat Delay Filters)

The filter responses seen till now have concentrated on the magnitude response. Due to this, these filters exhibit significant delay variation over the pass band. Thus all the fourier components of the input signal are not delayed by the same amount, which may lead to distortion of the output waveform. So for certain cases the requirement is to

have a constant time delay, i.e. phase shift that is linearly proportional to frequency, rather than a flat pass band.

Bessel filters are the types of responses which yield a maximally flat group delay. For a given number of poles, its magnitude response is not as flat, nor is its initial rate of attenuation beyond the -3dB cutoff frequency as steep as the Butterworth. So Bessel filters are used when the group delay flatness is more important than the magnitude response. The following graph shows the comparative group delay of Butterworth, Chebyshev and Bessel responses.

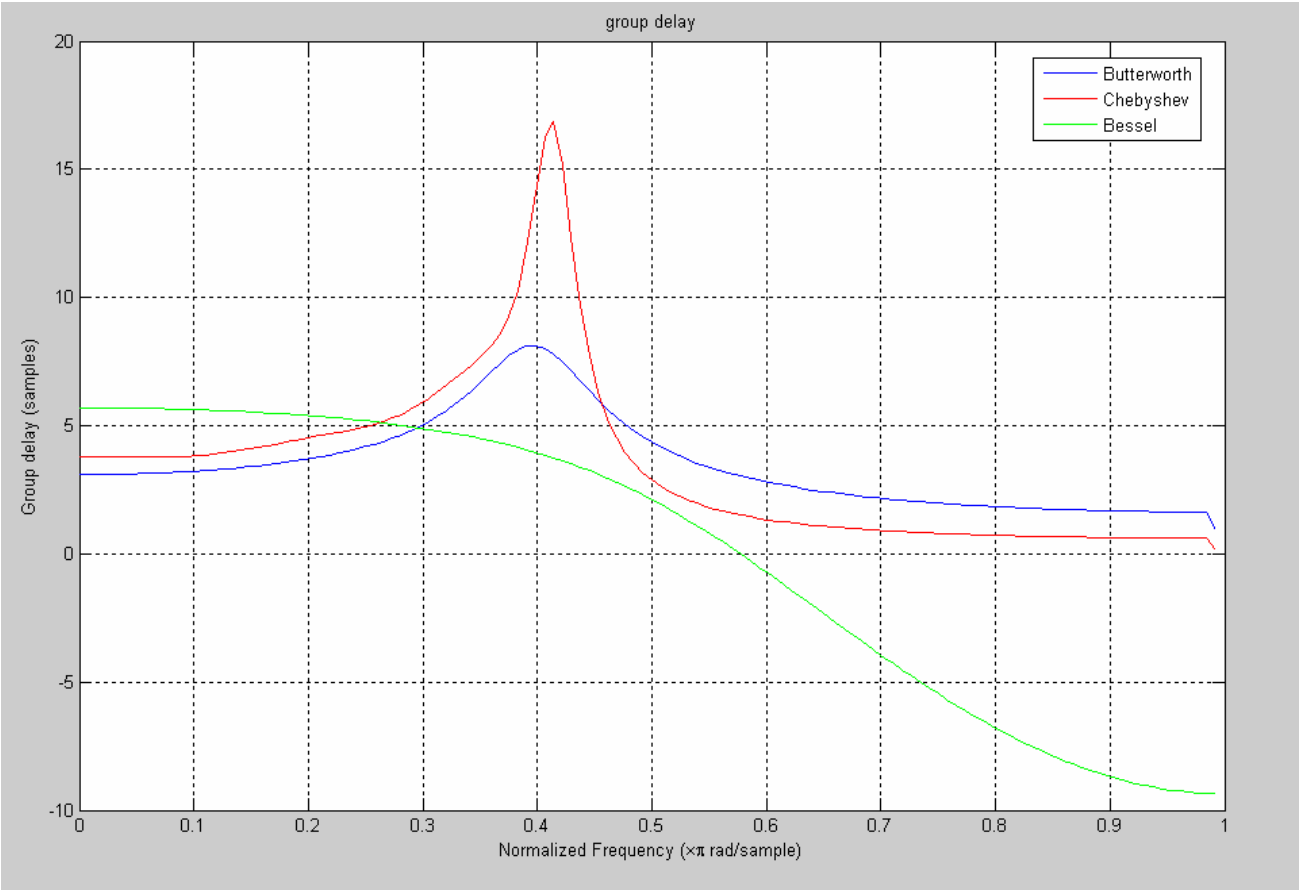

Figure A.4: Group Delay Comparison of Bessel, Butterworth and Chebyshev responses.

Appendix B

Result Plots

B.1 Hairpin Filter

B.1.1 Insertion Loss (S_{21} in dB)

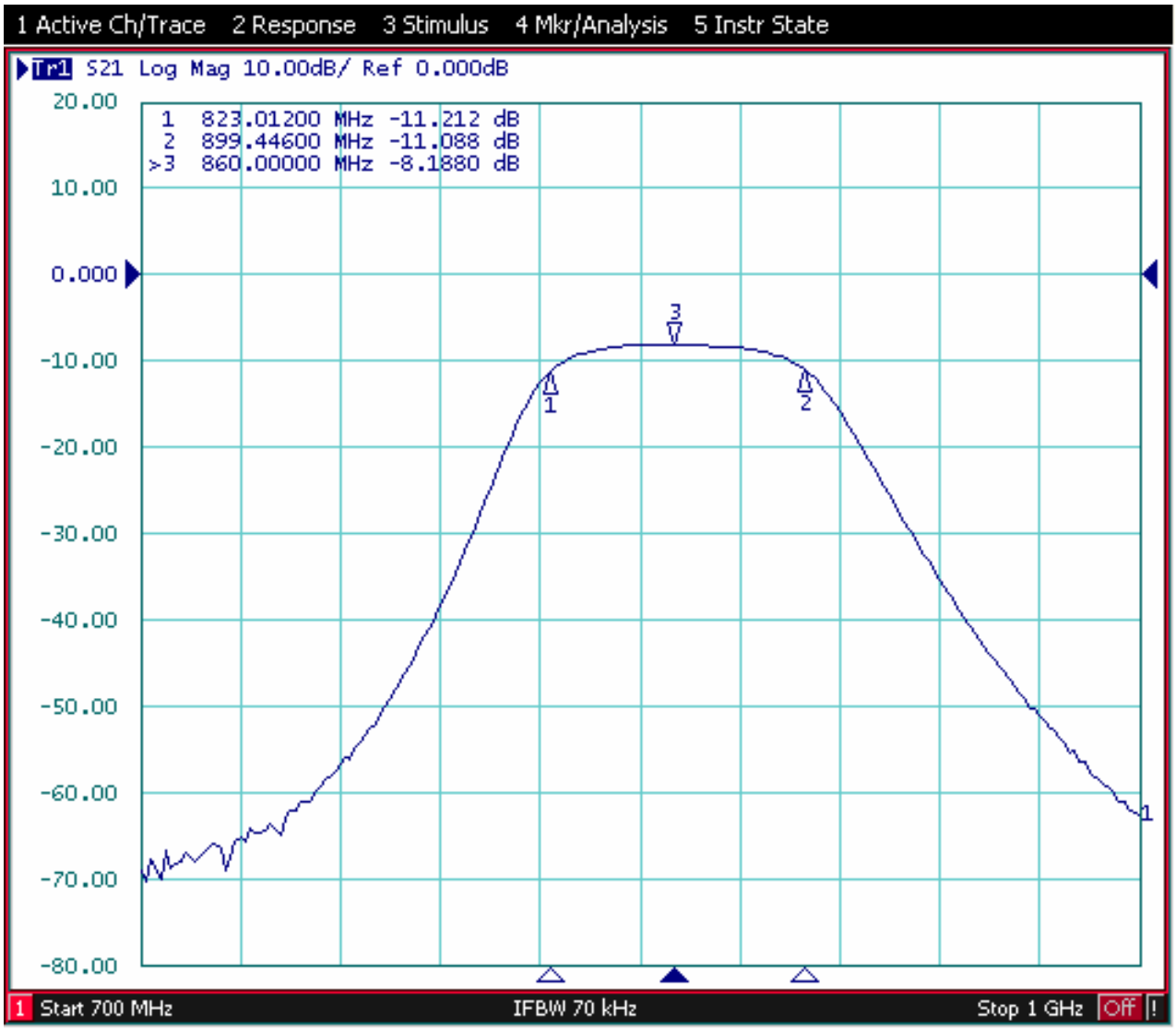

B.1.2 Return Loss (S_{11} in dB)

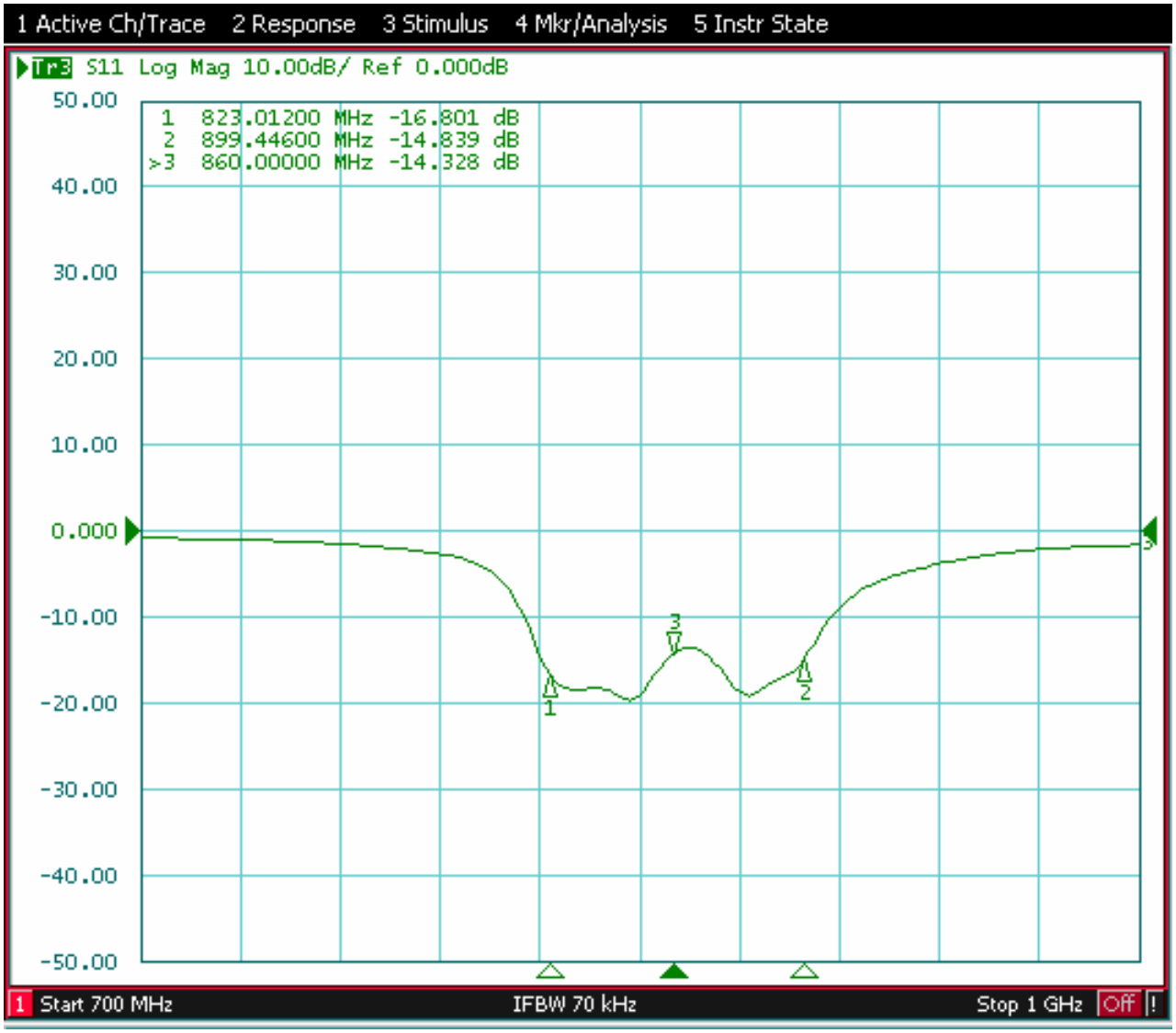

B.1.3 SWR

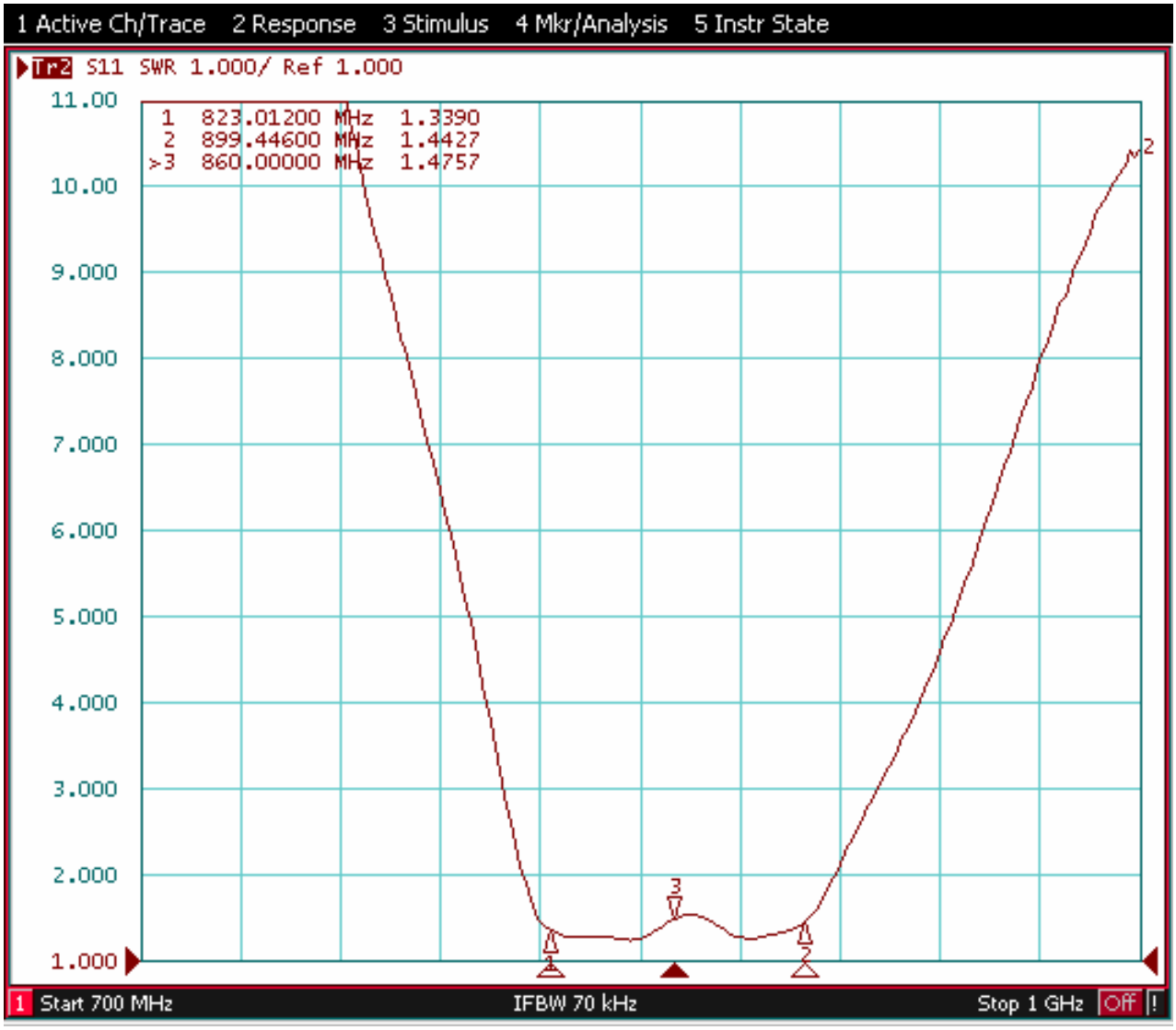
1 Active Ch/Trace
2 Response
3 Stimulus
4 Mkr/Analysis
5 Instr State
Tr2 S11 SWR 1.000/ Ref 1.000
1 823.01200 MHz 1.3390
2 899.44600 MHz 1.4427
>3 860.00000 MHz 1.4757
11.00
10.00
9.000
8.000
7.000
6.000
5.000
4.000
3.000
2.000
1.000
1 Start 700 MHz
IFBW 70 kHz
Stop 1 GHz
Off

B.1.4 Group Delay

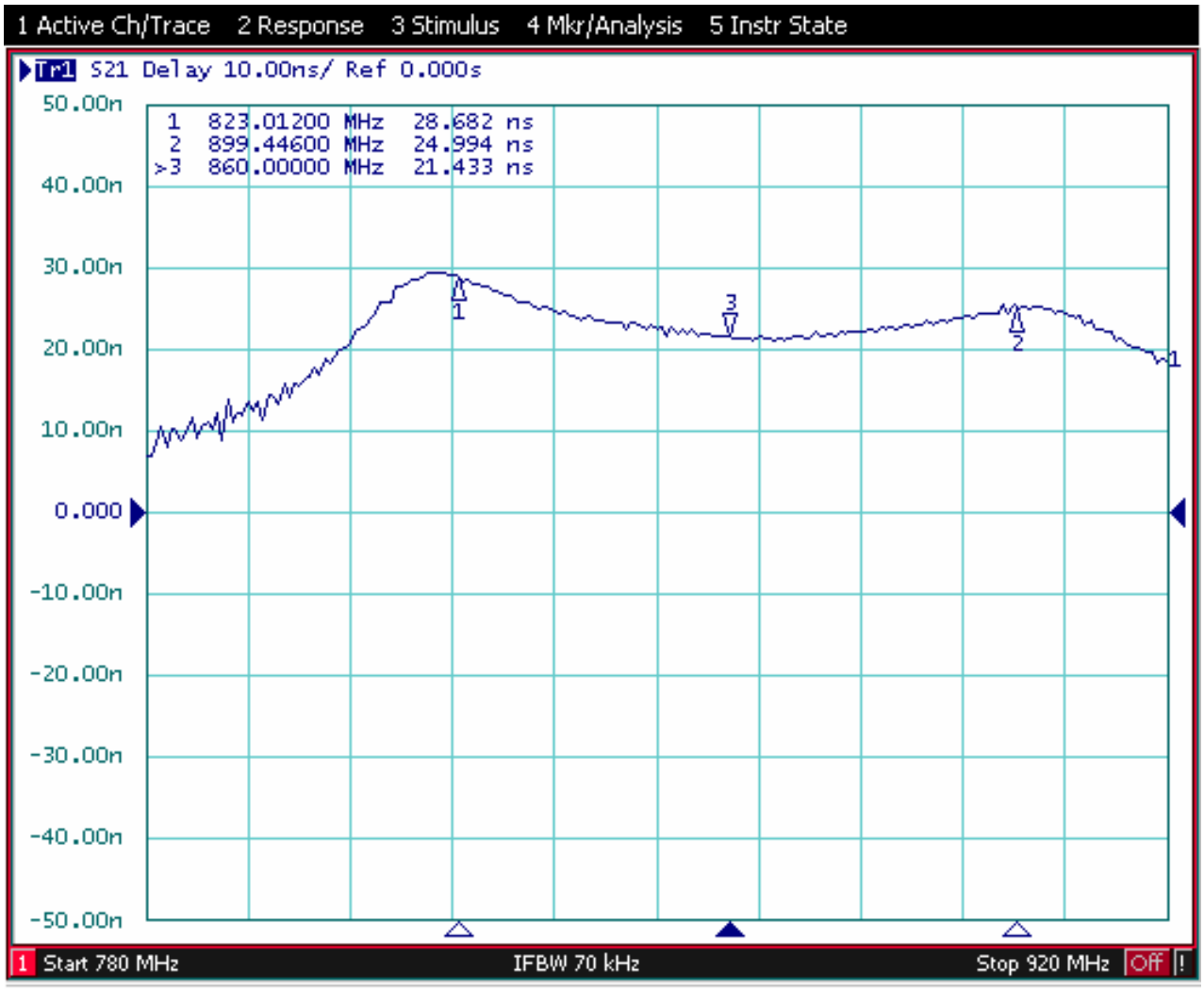

B.1.5 Wide Band Response

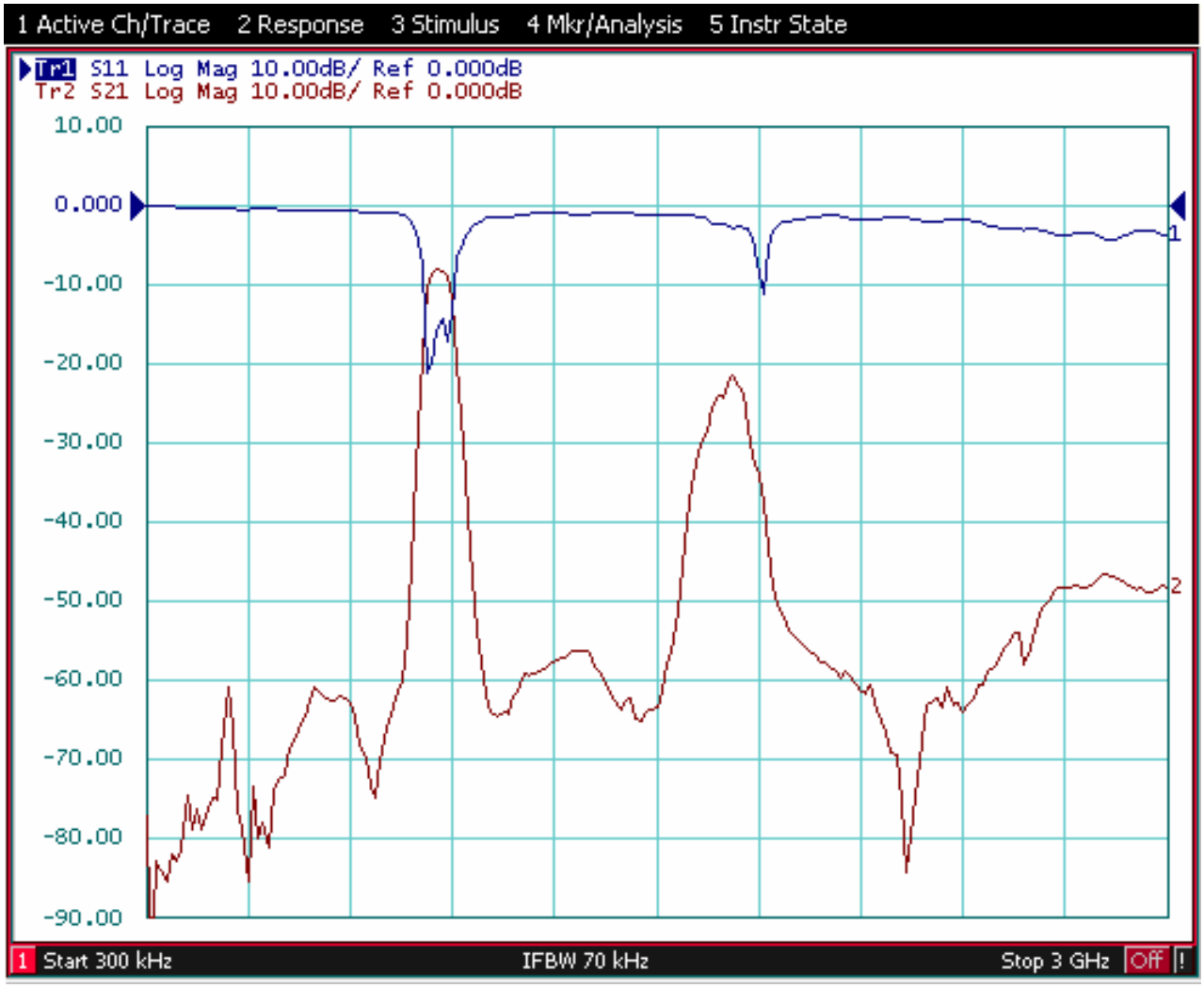

B.2 Open Loop, Cross Coupled Filter

B.2.2 Insertion Loss (S_{21} in dB)

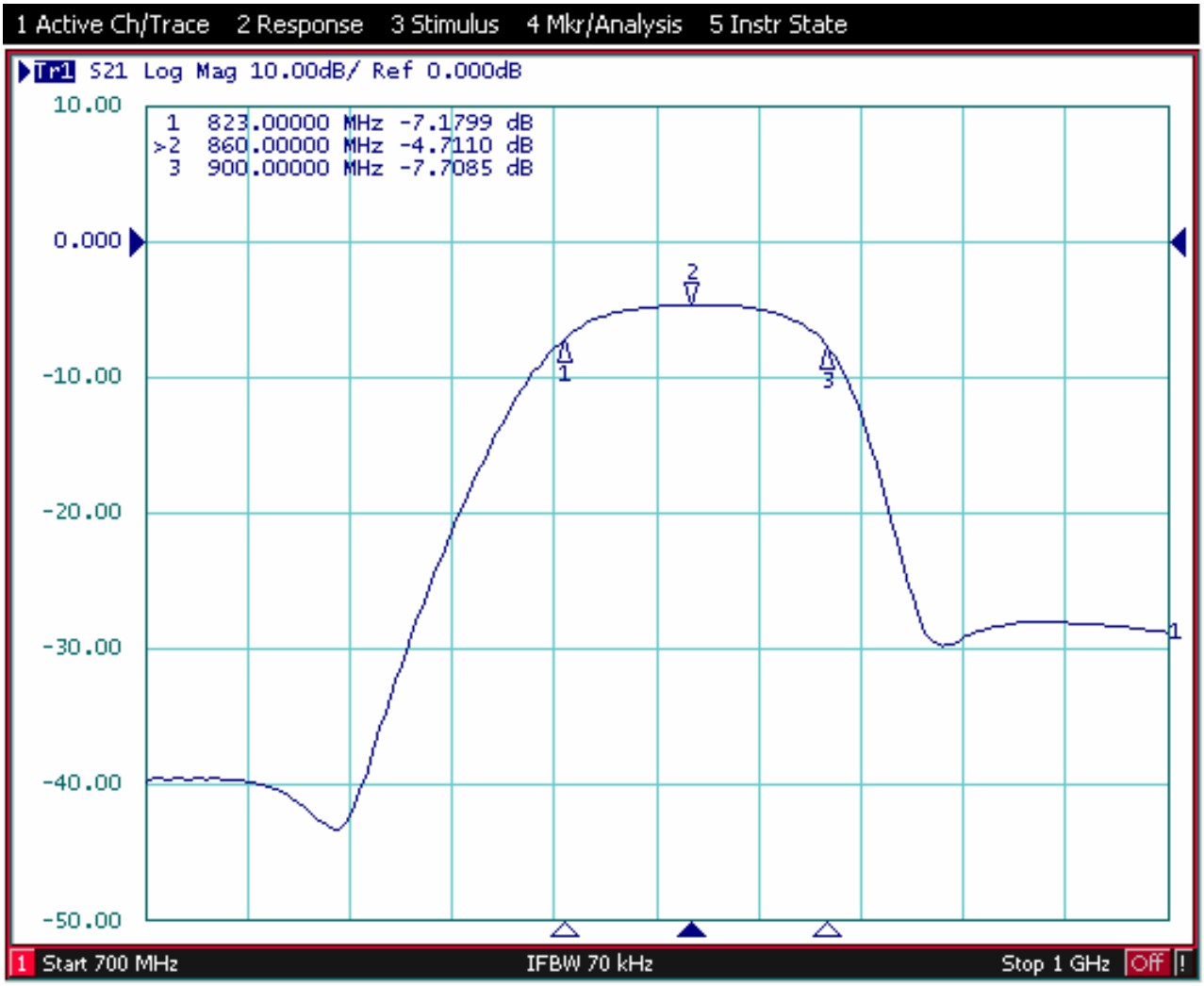

B.2.2 Return Loss (S_{11} in dB)

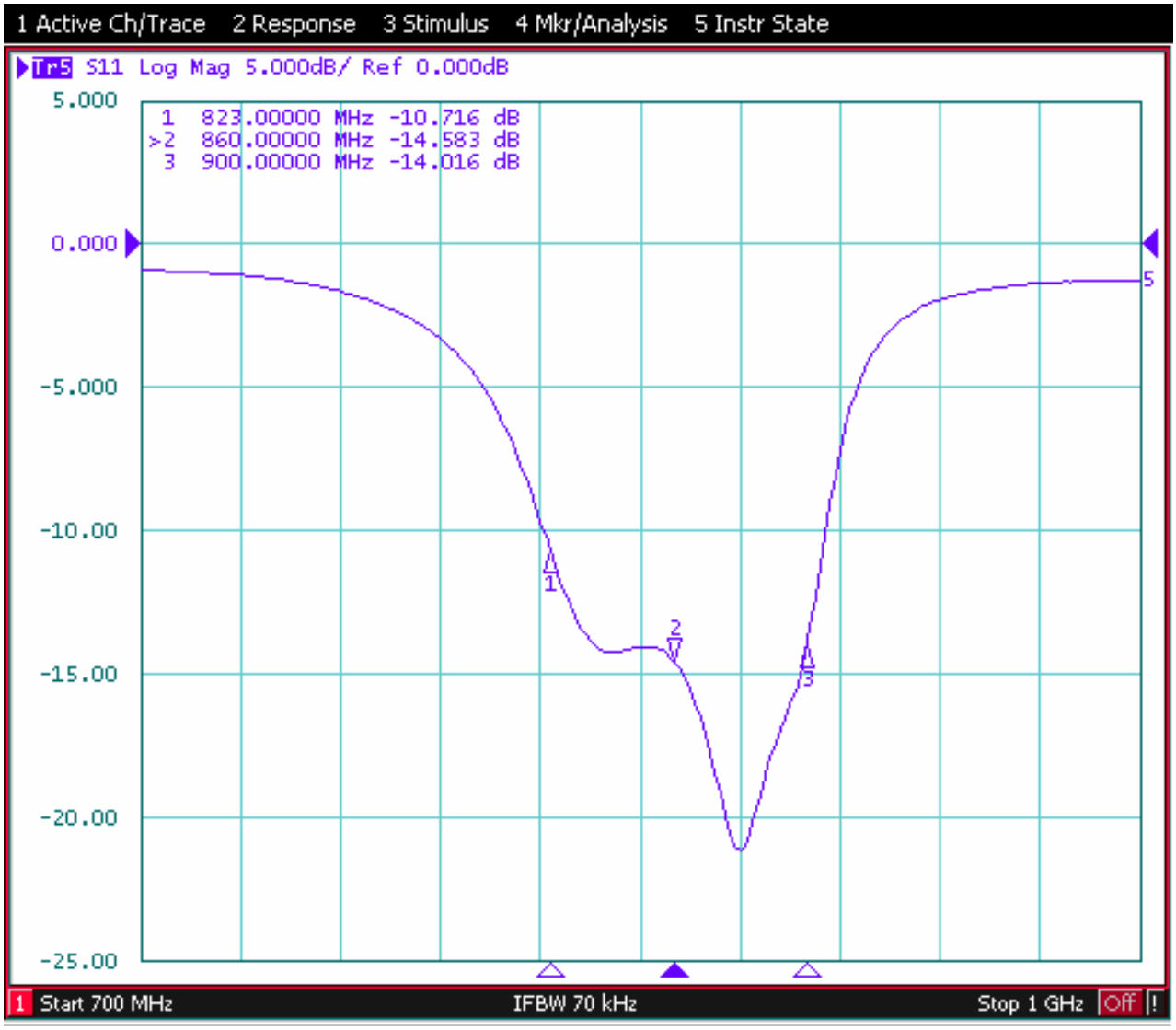

B.2.3 SWR

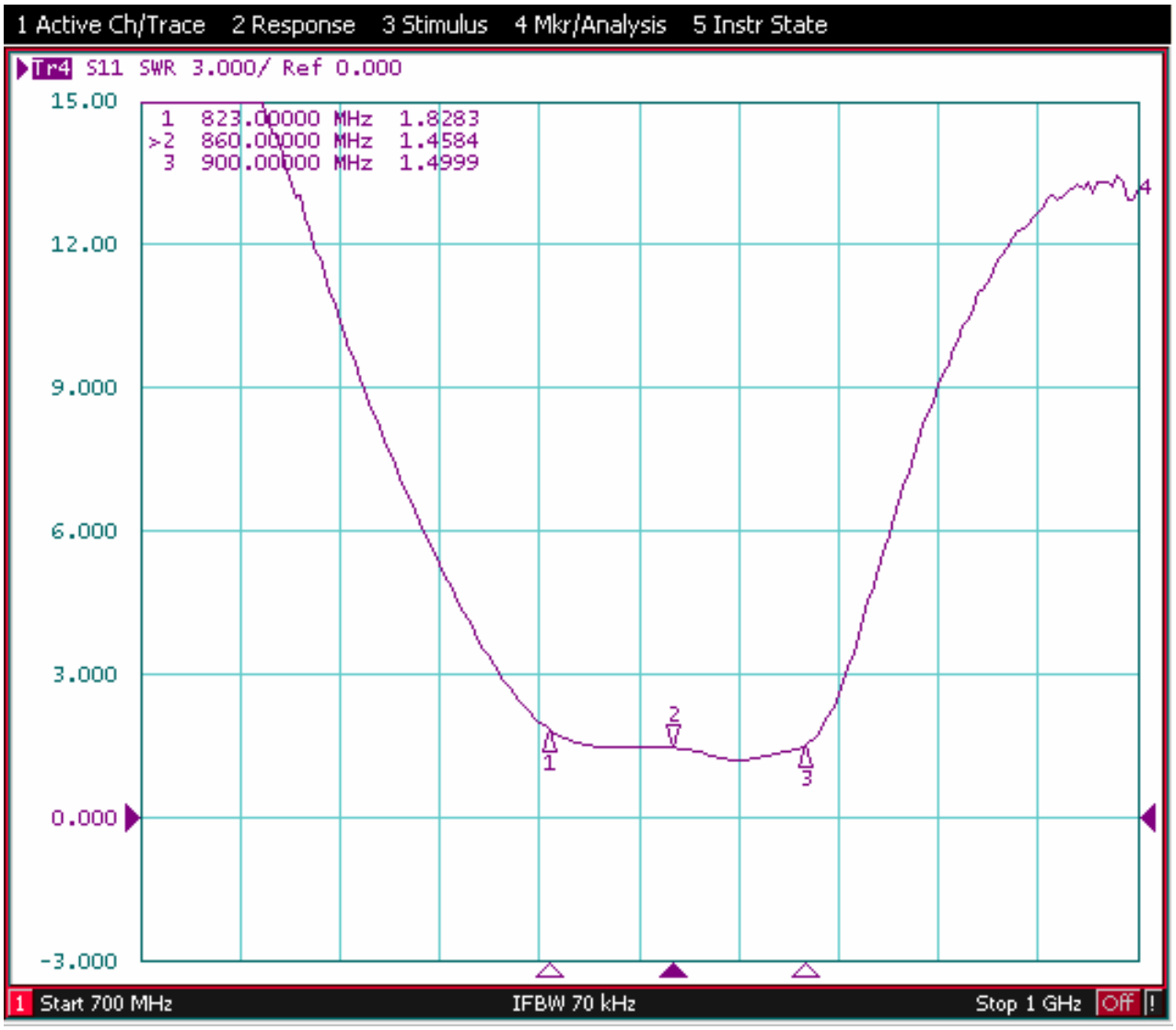
1 Active Ch/Trace
2 Response
3 Stimulus
4 Mkr/Analysis
5 Instr State
Tr4 S11 SWR 3.000/ Ref 0.000
1 823.00000 MHz 1.8283
>2 860.00000 MHz 1.4584
3 900.00000 MHz 1.4999
15.00
12.00
9.000
6.000
3.000
0.000
-3.000
1
2
3
4
1 Start 700 MHz
IFBW 70 kHz
Stop 1 GHz
Off

B.2.4 Group Delay

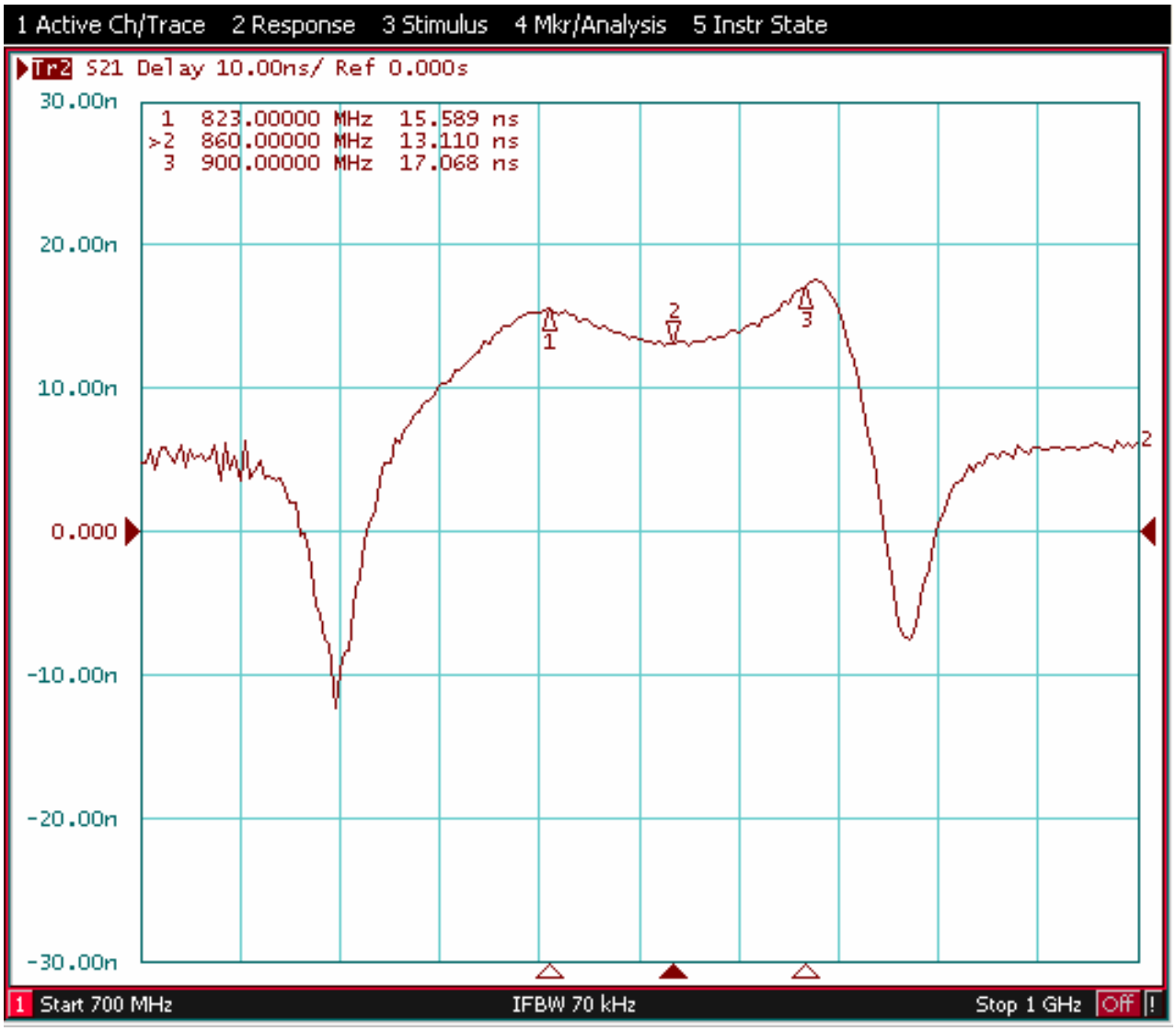

B.2.5 Wide Band Response